MALAN, DANIEL

ARRAYS OF CRYSTALLINE MEMBRANE ION-SELECTIVE ELECTRODES IN FLOW INJECTION POTENTIOMETRY

MSc UP 1997

Arrays of crystalline membrane ion-selective electrodes in flow injection potentiometry

by

Daniel Malan

Submitted in partial fulfilment of the requirements for the degree

MAGISTER SCIENTIAE

in the Faculty of Science
University of Pretoria
Pretoria
November 1997

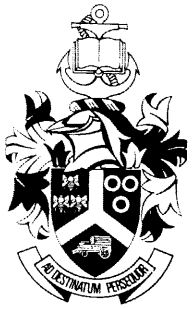

Arrays of crystalline membrane ion-selective electrodes in flow injection potentiometry

by

Daniel Malan

Leader: Professor Jacobus F. van Staden

Department of Chemistry

University of Pretoria

Degree: Magister Scientiae

SYNOPSIS

Using multiple low-cost detectors in flow injection analysis can reduce the cost per analysis. Ion-selective electrodes make good detectors, and electrodes with crystalline membranes often need little maintenance. The response of chloride, bromide, and iodide selective electrodes to the mutually interfering chloride and bromide are modeled by the Nikolskii equation. It is shown that, although the Nikolskii equation do not model the electrode potentials without bias, the precision of the predicted concentrations are determined more by the error propagation properties of the calibration procedure than by the lack of fit of the model to the experimental potentials.

Fluoride- and chloride-selective electrodes detect the non-interfering chloride and fluoride ions. The properties of a flow-injection system for the routine determination of fluoride and chloride were investigated and it was found that the flow-cell geometry, electrical earth connection, and streaming potentials influence the quality of analysis.

Reekse van kristalmembraan ioonselektiewe elektrodes in vloei-inspuit potensiometrie

deur

Daniel Malan

Leier: Professor Jacobus F. van Staden

Departement Chemie

Universiteit van Pretoria

Graad: Magister Scientiae

SAMEVATTING

Die gebruik van goedkoop meervoudige detektore in vloei-inspuit analise kan die koste per analise verlaag. Ioonselektiewe elektrodes is goeie detektore en dié met kristalmembrane verg dikwels min instandhouding. Die respons van chloried-, bromied-, en jodiedselektiewe elektrodes op die onderling steurende chloried- en bromiedione word gemodelleer met die die Nikolskii-vergelyking. Daar word aangetoon dat, hoewel die Nikolskii-vergelyking nie 'n model sonder sydigheid is nie, die presisie in die bepaling van konsentrasies meer afhang van die foutvoortplantingseienskappe van die kalibrasiemetode as die swak passing van die model by die elektrodepotensiale.

Fluoried- en chloriedselektiewe elektrodes reageer op die nie-steurende fluoried- en chloriedione. Die eienskappe van 'n stelsel vir die roetinebepaling van fluoried en chloried in drinkwater is ondersoek en daar is gevind dat die selgeometrie, die elektriese aardverbinding, en stroompotensiale die kwaliteit van die analise beïnvloed.

Table of Contents

Preface to:

Arrays of Crystalline Membrane Ion-Selective Electrodes in Flow-injection Potentiometry

Flow-injection analysis is an automatic sample manipulation technique, and its main purpose to reduce the time it takes to do a chemical analysis. Although the technique is flexible and inexpensive, it is hampered by being able to determine only one analyte at a time. One of the solutions to this problem is to use a flow injection system with multiple detectors. Potentiometric detectors are particularly suitable for use in detector arrays, because they are inexpensive and selective. This dissertation explores the use of an array of two crystalline membrane ion selective electrode as detectors in flow-injection analysis.

The first two chapters are introductory chapters. In combination they will provide the reader with an adequate background to understand the chapters on the experimental work.

Chapter 1 was written for the reader without a previous knowledge of flow-injection analysis. After reading it he will be able to follow a discourse on flow-injection analysis, and understand the diagrams that accompany discussions of the subject.

Chapter 2 is for the reader without a previous knowledge of potentiometry and ion-selective electrodes. It follows the shortest possible path from the general concept of an electrode to an expression for the potential generated by an ISE. The reader who has finished this chapter will know why the Nernst equation for the potential of an ISE takes the form it does, and together with Appendix 1 he will be able to see that it is founded on thermodynamics. He will also see how materials as diverse as PVC and glass are used in potentiometry, and will not confuse an ISE with a Class II electrode

The subject of Chapters 3 and 4 is the experimental work. The structures of these chapters reflect the way the work was done. For Chapter 3 the experimental work was

completed, and the results interpreted afterwards: The *Results* and the *Discussion* sections are separate. In Chapter 4 the experimental work was modified by the experience gained: here the *Results and Discussion* forms a single section, subdivided by experimental subject.

Chapter 3 explores the use and limitations of the calibration of electrodes for the mutually interfering species chloride and bromide. Because of the mutual interference a special calibration technique is used, and its implementation is explained in Appendix 2.

Analysers that uses electrode array detectors faces problems different from those with single electrode detectors. Chapter 4 explores the technical aspects of the use of electrode arrays. Chloride and fluoride are used as model compounds, although their determination are also of practical significance. These species do not interfere on each other's electrodes, so that no special calibration techniques are needed, but the chemistry is more complex.

ACKNOWLEDGMENTS

I thank Suzanne Pretorius, Danie Malan and Angelique Botha for the proofreading and constructive criticism of the manuscript.

Chapter 1

Flow-injection Analysis

1.1. Introduction

1.2. Dispersion

1.3. Future

1.4. References

1.1 INTRODUCTION

Flow-injection analysis is an automatic sample-manipulation and detection technique, based on the controlled partial dispersion of solutions in narrow-bore tubes. The term "flow-injection analysis" was coined in 1975 [1], and since then the technique became known as a fast, flexible and adaptable way of doing automatic wet chemical analysis.

The following components (Figure 1) are common to all flow-injection analysers:

- The *propulsion unit* propels a solution at a constant rate into a tube. The solution is called the *carrier solution*, and when it is in motion through the tube, it is known as the *carrier stream*.

- The *injection unit* intercalates a definite but variable volume of sample solution into this carrier stream.

- Carrying the sample, the carrier leaves the injection unit for what is called the *reactor*, where the sample partially disperses and chemical reactions take place.

- At the *detector*, the change in concentration of the analyte is detected as a change in a continuously recorded electronic signal.

In operation, the following happens: A continuous stream of carrier flows from the propulsion unit, through the injection unit, the reactor, and the detector to the waste container. The detector continuously monitors some property of the solutions flowing through it. While the carrier is flowing uninterrupted and the detector is giving a steady signal, the injection unit replaces a section of the carrier stream with sample solution. This *plug* of sample solution is swept along to the reactor, where the analyte present in the sample plug changes the measured property of the solution. When the plug reaches the detector, this change alters its response. The signal rises, then falls, as the sample

References on page - 11 -

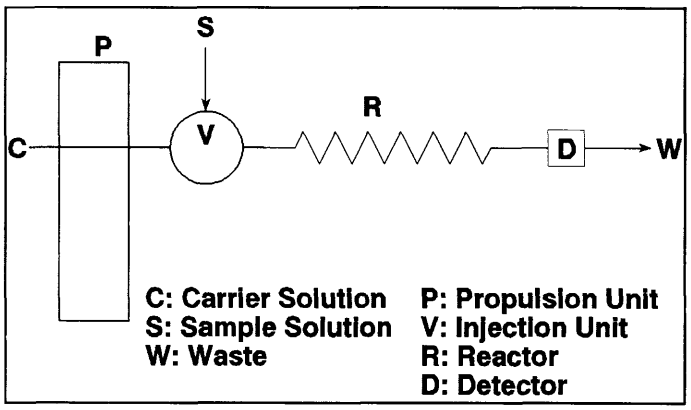

Figure 1 Symbols of components used in schematic diagrams of flow-injection systems.

plug is swept through the detector, to stabilize at the level it had before the injection. The signal is recorded, and afterwards some aspect of the *peak* (this is the usual name of the response/time curve) is measured. This measurement, when compared with a similar measurement of a standard sample's peak, indicates the analyte concentration.

The propulsion unit is usually a peristaltic pump, but compressed gas, syringe pumps, piston pumps or gravity feed can also be used.

Today the multiport rotary valve is the preferred injection device, but proportional and other novel injectors [2] are also sometimes used. The term 'flow-injection' is derived from the use of syringe injectors, but they are now obsolete.

The reactor can be a straight tube, a coiled or knotted tube, or a packed column. Sometimes an explicit reactor is omitted, but the tube leading to the detector will still cause dispersion.

Almost any of today's instruments can be used as a detector. The most favoured detectors are small and inexpensive, for the trend towards portable or mobile systems still continues, but FIA also makes it possible to increase the efficiency of complex and expensive instrumental techniques such as ICP-OES and ICP-MS. The most popular

References on page - 11 -

detection techniques are optical, with spectrophotometry by far the greatest component of that, followed by electrochemical techniques [3].

The above-mentioned components are found in all FI systems. Besides these, other special devices such as dialysers, solvent extractors, stills, gas exchangers, ion-exchange columns, and enzyme reactors can also be incorporated into the FI-manifold.

1.2 **DISPERSION**

When the sample plug is first placed in the carrier, it has a rectangular distribution. Once the plug starts moving under the laminar flow conditions prevailing in FI, it assumes a parabolic shape. The usual way to illustrate this is with a diagram like Figure 2. Diffusion and convection mix the sample plug with the carrier, dispersing it over a greater volume than it originally occupied. Controlled, limited *dispersion* is the basis of flow injection analysis.

Tyson [4] has pointed out the limitations of the kind of illustration shown in Figure 2. Given a tube diameter of 0.5 mm, the sample volume represented in the figure will be 0.83 $\mu\ell$. If the flow is 1 mℓ min^{-1}, then the average linear flow is 85 mm s^{-1}, and the linear flow in the centre of the channel is double that, 170 mm s^{-1}. The illustration therefore represents the state of laminar flow after 0.004 s. These figures do not, however, accurately reflect operational conditions. In typical FI applications the injected volume ranges from tens to hundreds of microlitres, and the time from injection may be more than a hundred seconds. The "hollow bullet" so often seen in diagrams should in fact be a long, hollow needle.

Dispersion is influenced by injected sample volume, carrier flow, reactor dimensions, and chemical reactions. It is quantified [8] by the ratio of the analyte concentration before dispersion to the analyte concentration after dispersion:

$$D = \frac{C_0}{C}$$

References on page - 11 -

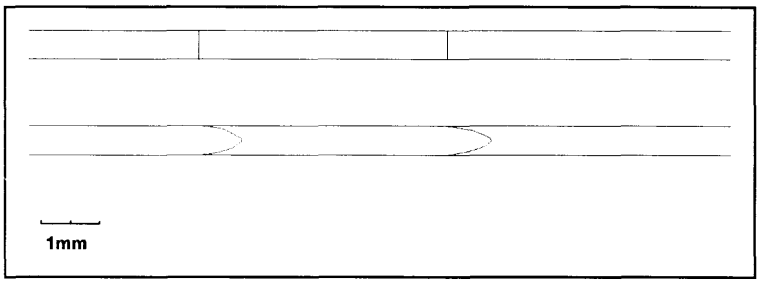

Figure 2. The distribution of a sample slug before (top) and during (bottom) dispersion.

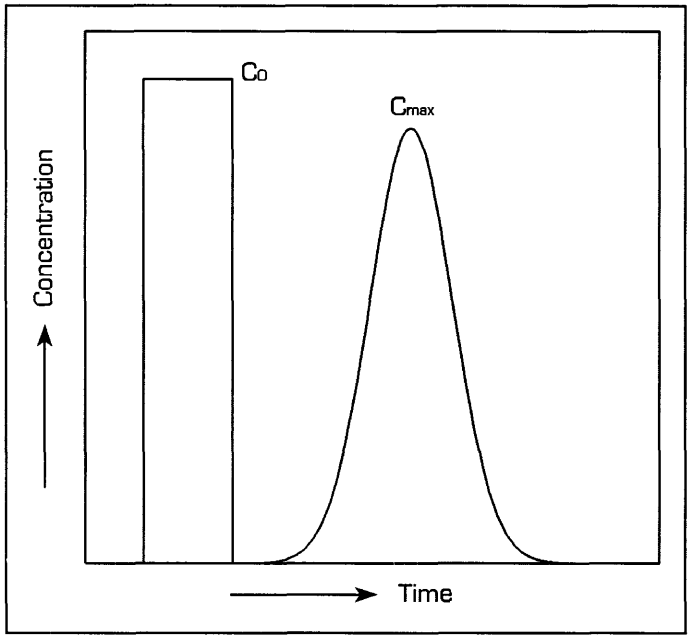

Figure 3 Photometric measurement of dispersion. C_0: Concentration of undispersed dye. C_{max}: Maximum concentration of dispersed dye.

If a flow-injection system uses photometric detection, dispersion in that system can be easily measured (Figure 3). Since absorbance depends on concentration, $C = kA$. Hence

$$D = \frac{k'A_0}{kA}$$

If Beer's law is valid, $k = k'$, and

$$D = \frac{A_0}{A}$$

While a dye solution is pumped through the system, the stable-state absorbance, A_0, is measured. A is the absorbance measured after injecting the same concentration of the

References on page - 11 -

dye into a carrier stream of water. D can then be calculated. If it is assumed that the diffusion constants of the dye and analyte are equal, the analyte must have the same dispersion. Each point on the time/concentration profile has its own dispersion, but the most convenient one to measure is D_{max}, the dispersion at the point of maximum concentration, C_{max}.

Dispersion is not easily measured in non-photometric systems, but it has been done, using voltammetric methods [5,6].

The desired properties of an FI-system is obtained by manipulating the components of the system that influences dispersion. As an aid to this Růžička and Hansen [3] formulated the following rules:

Rule 1. Changing the injected sample volume is a powerful way to change dispersion. An increase in peak height — and in sensitivity of measurement — is achieved by increasing the volume of the injected sample solution. Conversely, dilution of over-concentrated sample material is best achieved by reducing the injected volumes.

Rule 2. Limited dispersion value D is obtained by injecting a sample volume of minimum one $S_{½}$ into a manifold consisting of the shortest possible piece of a narrow-bore tube connecting the injection port and the detector. [$S_{½}$ is the volume of sample that has, after dispersion, a maximum concentration 50% of the steady-state concentration.]

Rule 3. The dispersion of the sample zone increases with the square root of the distance travelled through the tubular conduit and decreases with decreasing flow rate. Thus, if dispersion is to be reduced and the residence time is to be increased, the tube dimensions should be minimized and the pumping rate should be decreased. The most effective way to increase the residence time and to avoid further dispersion is to inject the sample into a flowing stream and stop

References on page - 11 -

the stream's forward movement, then resume pumping after a sufficient reaction time has elapsed.

Rule 4. Any continuous-flow system that includes a mixing chamber generates a larger dispersion and yields a lower measurement sensitivity than a corresponding channel without a mixing chamber. A system with a mixing chamber will also have a lower sampling frequency, unless the pumping rates are increased, which, in turn, require large sample and reagent volumes.

Rule 5. To reduce axial dispersion, which leads to a lower sampling frequency, the flow channel should be uniform without wide sections (which behave like poorly mixed chambers), and should be coiled, meandered, packed, or 3D-disoriented. Other types of sudden changes in direction of flow should also be included in the design.

Rule 6. To obtain maximum sampling frequency the flow system should be designed to have minimum $S_{½}$ and should be operated by injecting the smallest practical sample volume, S_v. FIA systems with minimum dispersion factor $\beta_{½}$ will require the least volume of reagent solution and will yield maximum sampling frequency in relation to residence time of the zone continuously moving through the channel. [$\beta_{½} = S_{½}/V_r$; V_r is the reactor volume]

Rule 7. Since any dispersed sample zone is composed of a continuous concentration gradient, a desired degree of dispersion can be conveniently selected by locating the analytical readout within that element of fluid that has a suitable dispersion coefficient.

Rule 8. All FIA titrations are based on peak width measurement, but not all peak-width measurements are FIA titrations. The difference is that FIA titrations are based on locating a pair of equivalence points by using indicator or self-indicating

References on page - 11 -

chemical reactions, while peak-width measurements rely on a time of flight of a dispersed zone measured at a selected level of detector response.

In the absence of a general theory of dispersion from which predictions about the performance and characteristics flow-injection systems can be made, this set of rules (or other, similar rules [7,8,9]) is the only guide to designing a FI system. These rules also illustrate the simplicity and flexibility of FIA.

1.3 **FUTURE**

"The most profound technologies are those that disappear. They weave themselves into the fabric of everyday life until they are indistinguishable from it" [10]

There are two ways in which FIA can disappear into the fabric of the everyday life of the analyst:

- The technique can be taken over by instrument manufacturers, so that every instrument carries it, either built-in or as an accessory.

- The elements of analysis using partial dispersion and incomplete reactions can be taught to students of analytical chemistry, so that these ideas can be used in solving problems in analytical chemistry, whenever it is most applicable.

These two ways are, of course, complementary: instruments with FIA built-in will teach analysts FIA, and analysts who know FIA will buy instruments that offer it as an option.

References on page - 11 -

1.4 **REFERENCES**

1. RŮŽIČKA J and HANSEN EH, Flow injection analysis. Part I: A new concept of fast continuous flow analysis. *Analytica Chimica Acta* (1975) **78**:145-157
2. BURGUERA JL, BURGUERA M, RIVAS C, DE LA GUARDIA M and SALVADOR A, Simple variable-volume injector for flow-injection systems. *Analytica Chimica Acta* (1990) 1 **234**:253-257
3. RŮŽIČKA Jaromir and HANSEN Elo Harald, *Flow Injection Analysis* 2nd ed. New York: Wiley (1988) xi, 498p. CHEMICAL ANALYSIS: A series... ISBN 0-471-81355-9
4. TYSON J, A Simple lecture demonstration of flow injection analysis. *Frezenius Zeitschrift für Analitische Chemie* (1988) **329**:675-677
5. KRISTENSEN EW, WILSON RL, WIGHTMAN RM, Dispersion in Flow Injection Analysis Measured with Microvoltammetric Electrodes. *Analytical Chemistry* (April 1986) 4 **58**:986-988
6. KAKIZAKI T, HASEBE K, YOSHIDA H, Evaluation of dispersion in a flow injection system by electrochemical detector and personal computer. *Frezenius Zeitschrift für Analitische Chemie* (1987) **326**:214-217
7. TYSON Julian F, Models for Dispersion in Flow Injection Analysis: Part 1. Basic requirements and Study of Factors Affecting Dispersion. *The Analyst* (April 1987) 4 **112**:515-521.
8. VALCÁRCEL M and LUQUE DE CASTRO MD, *Flow-injection analysis: principles and applications*. Chichester: Horwood (1987) 400p. Ellis Horwood Series in ANALYTICAL CHEMISTRY ISBN 0-85312-904-5
9. LI Y and NARUSAWA Y, Correlations among Dispersion Coefficient and FIA

Parameters Based on Experimental Data by Zone Circulating Flow-injection Analysis. *Analytical Sciences* (April 1994) 2 **10**:333-339

10. WEISER M, The Computer for the 21st Century, *Scientific American* (September 1991) p66-75

Chapter 2

Potentiometry and Ion-selective electrodes

2.1 INTRODUCTION

Potentiometry relates the concentration of a chemical species in solution with the electrical potential generated by a pair of electrodes in the same solution. This chapter explains the basic mechanism of the generation of this electrical potential, why ISEs are used and what they are, and how the concentration and the electrical potential is related. Some practical aspects of potentiometry are also discussed.

2.2 ELECTRODES

An *electrode* is a device, made of specific materials, that brings an electronic conductor into electrical contact with an ionic conductor. Electrodes are used in one of two ways: an electric potential can be applied to the electrode with the purpose of modifying the ionic conductor, or *electrolyte*. Alternatively, the potential generated by the interaction of the electrode and electrolyte can be exploited. Although the first option is of tremendous importance in science and technology, this discussion will concentrate on the potentials generated by electrodes. The basis of this aspect of electrodes is that at an interface between two materials charges are separated, and that this *charge separation* creates an electric field that can do work. Although the charge separation can occur at any interface, the aim here is to explain the origin of electrode potentials at the interface between a solid electrode and a liquid electrolyte.

There are two mechanisms by which charge separation is established at interfaces. The first assumes that charge transfer is allowed, the second that no charge is transferred.

- In the charge transfer approach, a non-fluid material (note the difference between fluid and liquid) containing ions is dipped into a solvent, containing the same ion species. The ions present in the material dissolve when brought into contact with the solvent, while the ions in the solvent desolvate and immobilise in the non-fluid material. Thus, a reversible reaction takes place. When the reaction reaches equilibrium the

References on page - 29 -

dissolution and immobilization take place at equal rates. The counter-ions will nót dissolve and immobilize at the same rate. This produces a nett charge on the surface of the body, and a layer of countercharge in the electrolyte.

- When no charge transfer across the interface is allowed, a separation of charge will still be established. This alternative model describes the ions in solution with their solvent spheres. When an interface is present, the forces on the solvent molecules become non-isotropic. This changes the number of solvated ions near the interface, causing a nett charge to build up in this region. An opposite charge is induced at the other side of the interface. In short, anisotropy in dispersion forces causes a partial charge separation.

Since charge transfer is always to some extent possible, both these processes take place simultaneously and their effects cannot be separated.

This is probably the simplest possible description of how the "electric double layer" is established. The exact structure of the double layer depends on the electrode material and the composition of the solution contacting it. Overall, however, the following features are believed to be found in most electrode interfaces:

The compact layer

It consists of:

The Inner Helmholz Layer

This is the layer of unsolvated ions and dipole solvent molecules closest to the interface. The ions will desolvate only if they have a greater affinity for the electrode than for the solvent molecules. These ions and solvent molecules are held in place by chemical forces (*i.e.* electric forces on a quantum scale.) The plane through the centre of the ions is called the inner Helmholz plane, abbreviated IHP.

References on page - 29 -

The Outer Helmholz Layer

This is the layer of solvated ions closest to the electrode surface. These solvated ions are held in place by electrostatic forces. The plane through the centres of these solvated ions is called the outer Helmholz plane (OHP).

The diffuse layer

Because of the thermal motion of ions, limited movement away from the interface can be expected. This motion causes the layer to extend into the electrolyte, decreasing in density as the distance from the interface increases. When the electrode material is not an electronic conductor a similar diffuse layer is found inside the electrode.

When the material on the solid side of the interface is shaped and combined with other materials so that it contacts an electronic conductor, the resulting device is an *electrode*.

Dahmen [1] uses the classification of electrodes illustrated in Figure 1. If the solid part of the interface is itself an electronic conductor, electron transfer alone is responsible for the potential differences, and the electrode is called a *normal electrode*. If ion-exchange is the source of charge separation, the electrode is called a *membrane electrode*. (The term membrane is used because the high electrical resistance of ion-exchange materials limits the thickness of the measuring element that can be used.) Membrane electrodes require at least one additional interface to complete the connection between the electronic conductor and the electrolyte.

Normal electrodes are used in analytical techniques such as polarography and electrogravimetry, and faradic techniques in general. Because normal electrodes are subject to contamination and interference by redox agents, the vast majority of

References on page - 29 -

potentiometric measurements are made with membrane electrodes. Membrane electrodes are also known as ion-selective electrodes.

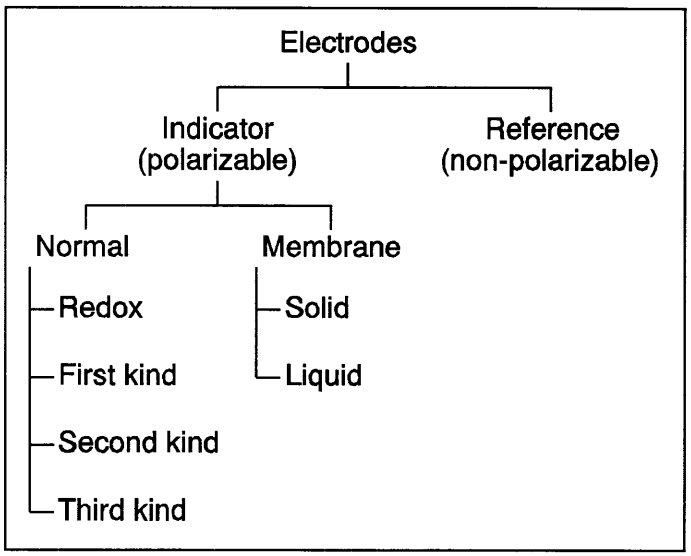

Figure 1. Classification of electrodes

References on page - 29 -

2.3 ION-SELECTIVE ELECTRODES

With ion-selective electrodes, the work that can be done by the electrode is measured to gain information on the composition of the electrolyte.

The Analytical Chemistry Division of IUPAC recommends [2] the following definition of ion-selective electrodes: these are electrochemical sensors, the potentials of which are linearly dependent on the logarithm of the activity of a given ion in solution. Such devices are distinct from systems which involve redox reactions (Class I and II electrodes).

The IUPAC [2] recommends the following classification of ion-selective electrodes, illustrated in Figure 2. Dahmen [1] classified all these as membrane electrodes.

A. Primary electrodes

1. *Crystalline electrodes* may be homogeneous or heterogeneous.

   a. *Homogeneous Membrane Electrodes* are ion-selective electrodes in which the membrane is a crystalline material.

      It can be a single-crystal (*e.g.* LaF_3) or
      monocrystalline (*e.g.* Ag_2S) or
      polycrystalline (*e.g.* AgI/Ag_2S)

   b. *Heterogeneous Membrane Electrodes* are formed when an active substance, or a mixture of active substances, is mixed with an inert matrix, such as silicone rubber or PVC, or placed on hydrophobized graphite, to form the sensing membrane that is heterogeneous in nature.

2. *Non-crystalline electrodes*. In these electrodes a support, containing an ionic (either cationic or anionic) species or an uncharged species, forms the ion-selective membrane, which is usually interposed between two aqueous solutions. The support can be either porous or non-porous. These electrodes exhibit a response due to the presence of the ion-exchange material in the membrane.

   a. *Rigid matrix electrodes* (*e.g.* glass electrodes) are ion-selective electrodes in which the sensing membrane is a thin piece of glass. The chemical

References on page - 29 -

composition of the glass determines the selectivity of the membrane. Hydrogen-ion selective electrodes and monovalent cation-selective electrodes are included in this group.

b. *Electrodes with a mobile carrier:*

(1) Positively charged carrier - When bulky cations are dissolved in a suitable organic solvent and held on an inert support, they provide membranes that are sensitive to changes in the activity of anions.

(2) Negatively charged carrier - When complexing agents or bulky anions are dissolved in a suitable organic solvent and held in an inert support, they provide membranes that are sensitive to changes in the activity of cations.

(3) Uncharged carrier - Electrodes based on solutions of molecular carriers of cations that can be used in membrane preparations that show sensitivity and selectivity to certain cations.

B. Sensitized ion-selective electrodes

1. *Gas sensing electrodes* are sensors composed of an indicating and a reference electrode that use a gas-permeable membrane or an air-gap to separate the sample solution from a thin film of an intermediate solution, which is either:

held between the gas membrane and the ion-sensing membrane of the electrode, or

placed on the surface of the electrode using a wetting agent (*e.g.* air gap electrode).

This intermediate solution interacts with the gaseous species in a way that produces a change in a measured value (*e.g.* pH) of the intermediate solution. This change is then sensed by the ion-selective electrode and is proportional to the partial pressure of the gaseous species in the sample.

2. *Enzyme substrate electrodes* are sensors in which

- an ion-selective electrode is covered with a coating containing an enzyme that causes the reaction of an organic or inorganic substrate to produce a species to which the electrode responds.

References on page - 29 -

or

- an ion-selective electrode is covered with a layer of substrate that reacts with the enzyme to be assayed.

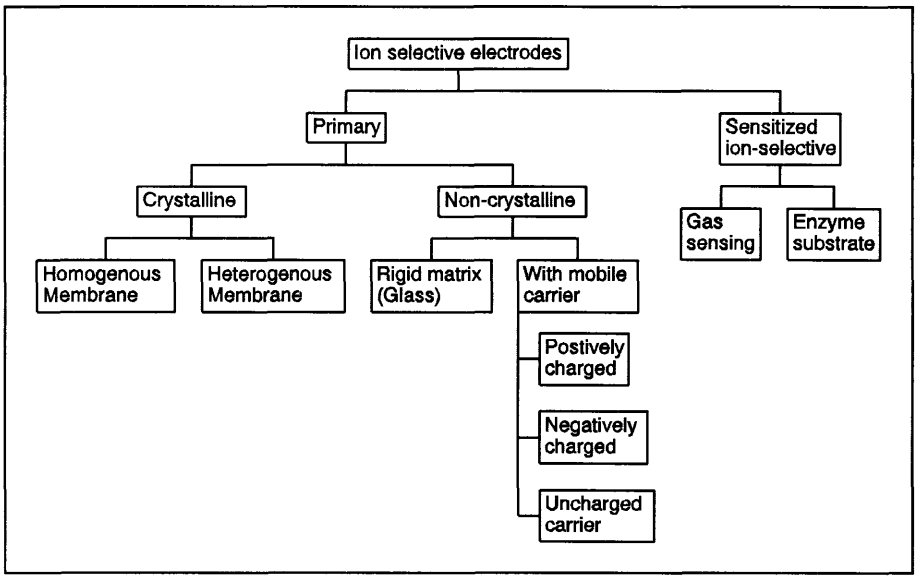

Figure 2. Recommended classification of ion-selective electrodes [2].

Another class of detectors, closely related to the above is known as ISFETs, or ion sensitive field-effect transistors. These are FETs in which the gate electrode is replaced by a thin layer of ion-exchange material. The charge separation at the surface of the ion-exchange material controls the drain current. Various uses for ISFETs have been discovered, but they are not discussed in this paper.

References on page - 29 -

2.4 ELECTRODE POTENTIALS

The potential difference between two points *a* and *b* is defined by the line integral of the electric field.

$$V_{ab} = V_a - V_b = \int_a^b \boldsymbol{E} \cdot d\boldsymbol{l}$$

The instrumentation available to chemists can measure potential differences in two metallic conductors only. Therefore, any measurement of potentials in electrolytes requires at least two electrodes.

The most useful line along which to calculate the line integral runs from the first contact of the voltmeter, through the metallic conductor, the first electrode, the electrolyte, the second electrode, and through the metallic conductor to the second contact of the voltmeter. The electric field inside the conductors is zero, and the only region where the field change is at the electrode interfaces. The integration then boils down to a summation of interfacial potential differences.

The main contribution to the electric field is the charge separation established by ion-exchange, discussed in Paragraph 2.2 above. A lesser contribution is by the oriented solvent dipoles in the inner Helmholz layer of the electrode-electrolyte interface, causing what is known as the surface potential difference, $\Delta\chi$. The charge separation and the dipole layer density depend in different ways on the composition of the electrode and electrolyte. It is customary to write an expression describing these different influences on the total potential difference:

$$\Delta\phi = \Delta\psi + \Delta\chi$$

$\Delta\psi$ is known as the outer- or Volta potential difference, and represents the potential difference experienced by ions in the electrolyte.
$\Delta\phi$ is known as the inner- or Galvani potential difference, and is the potential difference experienced by electrons in the electrode. The Galvani potential difference is the

References on page - 29 -

potential difference measured by moving coil- and operational amplifier voltmeters. (Oscilloscopes measure the Volta potential of the region between the deflection plates, but because the plates operate in a vacuum the surface potential is considered negligible, and this potential is considered equal to the Galvani potential of the plates.)

The surface potential limits the accuracy of information about the composition of the electrolyte gathered by electrode. Few chemists consider the influence of the surface potential in calculations, because it is smaller than other sources of uncertainty, and during practical measurement it is largely cancelled out by an opposite surface potential at the other electrode.

The influence of the chemical composition of an electrolyte on electrode potential can be calculated by considering the energy involved. The maximum non-expansion work a substance can do per mole is given by the chemical potential:

$$\mu_i = \mu_i^\circ + RT \ln a_i$$

(See Appendix 1 for a derivation of this expression)
Charged species however, can do more work, depending on the electrical potential at the position of the substance. A term compensating for this must be introduced:

$$\mu_i = \mu_i^\circ + RT \ln a_i + z_i F\phi$$

where ϕ is the electrical potential of the solution, z_i the charge of the ion, and F the faraday constant. This is known as the *electrochemical potential.*

Consider an ion-exchange membrane between two electrolytes with a common ion *i* within the following measuring cell:

References on page - 29 -

External reference electrode (of choice)	Aqueous solution S with variable ion activity a_i^S	ion-exchange membrane n with respect to ion i	aqueous solution S_0 with fixed ion activity a_i^{S0}	Internal reference electrode (e.g. Ag/AgCl)

then the potential profile of the membrane ISE can be depicted by Figure 3 and represented by

$$\Delta E = \epsilon_{m_0} - \epsilon_S = (\epsilon_{m_0} - \epsilon_{S_0}) + (\epsilon_{S_0} - \epsilon_n) + (\epsilon_n - \epsilon_S)$$

where ϵ_{m_0} is the potential of the internal reference electrode and ϵ_n is the potential of the membrane.

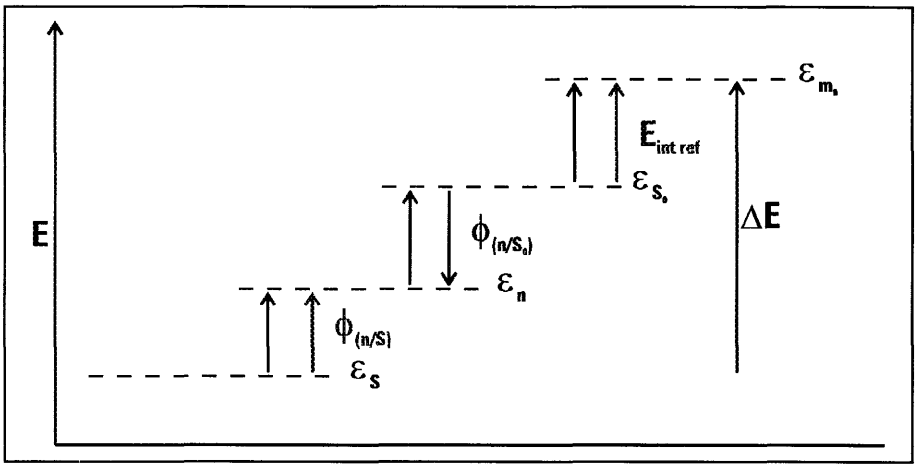

Figure 3 Potential profile of a membrane ISE

We assume that between the membrane phase (n) and the solutions (S and S_0) no diffusion potentials occur, *i.e.* the potential differences $\phi_{(n/S)}$ and $\phi_{(n/S_0)}$ are caused by ion-exchange activity only. Further, all phases are considered to be homogeneous so that $\mu^0_{(n)}$ is constant within the membrane and $\mu^0_S = \mu^0_{S_0}$ within the solutions. Let us consider the simple system of selective indication of ion A with charge z_A. At the interface between the outer solution and the membrane the electrochemical potentials of the adjacent phases under equilibrium conditions must be equal, therefore we can write

$$\mu^0_{A(n)} + RT \ln a_{A(n)} + z_A F \phi_{(n)} = \mu^0_{A(S)} + RT \ln a_A(S) + z_A F \phi_{(S)}$$

References on page - 29 -

so that

$$\phi_{(n/S)} = \phi_{(n)} - \phi_{(S)} = \frac{1}{z_A F}(\mu^0_{A(n)} - \mu^0_{A(S)}) + \frac{RT}{z_A F} \ln (a_{A(n)}/a_{A(S)})$$

and with

$$A^0_A = \mu^0_{A(n)} - \mu^0_A(S)$$

$$\phi_{(n/S)} = \frac{A^0_A}{z_A F} + \ln(\frac{A_{A(n)}}{A_{A(S)}})$$

According to the potential profile in Figure 3 the potential of the ISE is

$$\Delta E = \epsilon_{m_0} - \epsilon_S = (\epsilon_{m_0} - \epsilon_{S_0}) + (\epsilon_{S_0} - \epsilon_n) + (\epsilon_n - \epsilon_S)$$

and hence

$$E = E_{int\ ref} - \phi_{(n/S_0)} + \phi_{(n/S)} = E_{int\ ref} + \phi_{(n/S)} - \phi_{(n/S_0)}$$

Since

$$\phi_{(n/S)} - \phi_{(n/S_0)} = (\frac{A^0_A}{z_A F} + \frac{RT}{z_A F} \ln (\frac{a_{A(n)}}{a_{A(S)}})) - (\frac{A^0_A}{z_A F} + \frac{RT}{z_A F} \ln (\frac{a_{A(n)}}{a_{A(S_0)}}))$$

$$E = E_{int\ ref} + \frac{RT}{z_A F} \ln (a_{A(S_0)}) - \frac{RT}{z_A F} \ln (a_{A(S)})$$

According to this the standard potential of the ISE depends on the specific choice of the internal reference electrode (*e.g.* Ag/AgCl) and on the fixed *A* concentration of the filling solution, so that

$$E_{ISE} = E^0_{ISE} - \frac{RT}{z_A F} \ln (a_A)$$

Electrodes with crystalline membranes (those based on Ag_2S being a good example) can be made in the *solid state* form. In such a form the internal reference electrode is omitted, and the electronic conductor touches the membrane directly, often cemented to it with a metal-loaded epoxy. Buck [3] argues convincingly that the expression stays the same, whether the charge transfer is by electron or by mobile metal ions.

References on page - 29 -

This derivation of electrode potential is for the ion exchange of a single ion: it is the case for the ideal ISE. When more than one ion species can exchange with ions in the electrode membrane, all of them will contribute to the electrode potential. The ion of interest is known as the *primary ion*. Other ions that also contribute to the potential are *interfering* ions. To describe the contribution to the electrode potential by the interfering ions B, C *etc.* the modified Nernst equation is used:

$$E = E^\circ + \frac{RT}{z_A F} \log[a_A + K_{AB}(a_B)^{z_A/z_B} + K_{AC}(a_C)^{z_A/z_C} + \ldots]$$

The constants K_{ij} are known as the *selectivity coefficients*. The smaller the selectivity coefficients are, the more selective the electrode is. This equation is often called the Nikolskii or Nikolskii-Eisenmann equation.

References on page - 29 -

2.5 **POTENTIOMETRY: the measurement of electrode potentials**

Potentiometry is an instrumental analysis technique, and involves measuring the potentials of electrochemical cells acting reversibly. Its relationship with other techniques is illustrated in Figure 4. The vast majority of potentiometric measurements are made with ion-selective (inert) electrodes.

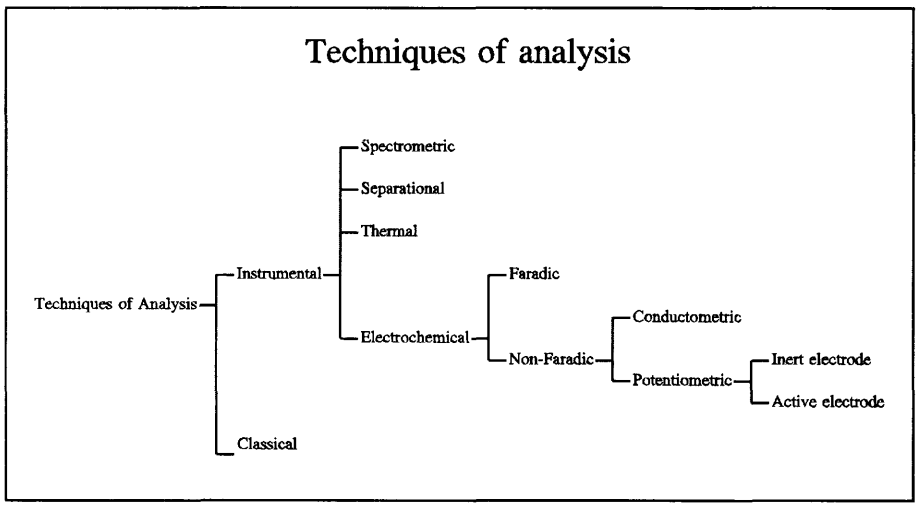

Figure 4. The relationship between potentiometry and other techniques of analysis.

The basis of potentiometry with ion-selective electrodes is that the potential of an electrode depends on the constitution of the solution in contact with it. More specifically, an ion-selective electrode gives a voltage proportional to the logarithm of the concentration of a specific species [2].

A cell acts reversibly only when no current is drawn from it. The measurement of reversible cell potentials must therefore be made under zero-current conditions. This criterium can be met in only one way: the potential to be determined must be balanced by an outside potential that can be measured accurately. Another option, however, is available. If a very small current is drawn from the cell, the equilibrium will not be significantly disturbed. The potential drop (iR drop) of this current over a standard resistor can be measured to give the voltage of the cell. This second method, although not as

References on page - 29 -

accurate as the compensation method, is so convenient that it is the preferred method for making analytical measurements.

As noted above (Paragraph 2.4) at least two electrodes are needed to investigate the potentials developed at electrolyte/electrode interfaces. The electrode called the *indicator*, *test* or *working electrode* generates the potential of interest. If this potential is to have a meaning, the potential at the other electrode must be known, or at least stable. This other electrode is therefore called the *reference electrode*. The reference electrode is normally a non-polarizable [4] electrode. The best known of these are the calomel (Hg/Hg_2Cl_2) and silver chloride (Ag/AgCl) electrodes.

In potentiometry the ionic strength of samples and standards are usually increased by the addition of a salt that does not interfere with either the ISE or the reference electrode. Under these conditions the analyte ion activities in samples and standards are constant and proportional to the concentration. (See Appendix 1 for an explanation of the relationship between ion activity and ionic strength.)

Another reason for working at high ionic strengths, explained by Atkins [4], is fairly simple: the aim of measurement is to know the activity or concentration of ions in solution. The diffuse layer of countercharge changes the ionic activity near the electrode surface. Any measurement of activity will therefore not represent bulk solution activity. The obvious and usual way of dealing with this is to work at high ionic strengths. The diffuse countercharge layer is then forced to be very thin, and any local effects are swamped by the surplus of inert ions.

A more complex reason for the use of a high ionic strength solution is the avoidance of electrokinetic phenomena, especially streaming potentials. The compact layer of the electric double layer sticks tightly to the electrode surface, and motion in the electrolyte will not disturb it. A *plane of shear* can be defined as the outer plane of the layer of molecules that will not be disturbed by motion in the bulk of the liquid. The potential at the plane of shear is called the *zeta potential*, and it depends on the extent of the

References on page - 29 -

diffuse layer beyond the plane of shear. In the diffuse layer there is an excess of charge. When the electrolyte moves there is a motion of the portion of the diffuse layer that extends beyond the plane of shear. This causes an additional separation of charge, and the potential associated with it is called the *streaming potential*. The streaming potential obviously depends on the electrolyte flow and the zeta-potential. Increasing the ionic strength has the effect of reducing the thickness of the diffuse layer. (The mechanism of this contraction is described by the Debye-Hückel theory.) A thinner diffuse layer means that the zeta-potential decreases, which decreases the streaming potential for a given flow pattern.

A detail that must be kept in mind during practical potentiometry is known as the *junction potential*. It arises when two electrolytes containing different concentrations or different species of ions are brought into contact. The different rates of diffusion cause a charge separation, leading to a potential difference. Most commonly, the junctions of different solutions are found between the filling solution of the reference electrode and the test solution. The junction potential is often said to be reducible to less than 2 mV. At that level it will not reduce accuracy much. Usually it is only necessary to keep it constant; its effect is then lumped with the other unknowns in the calibration constants.

The following quotation comes from Cammann [5], and indicates the importance of sample preparation when using ion-selective electrodes in chemical analysis:
"Ion-selective electrodes respond to the activity of the indicated ion in solution. With the exception of their use as titration endpoint indicators, they require calibration with a standard solution of known activity. In the determination of concentrations, the error depends in large part on the validity of the assumed equality and constancy of activity coefficients in the sample and calibration solutions."[his italics]

In flow-injection systems the sample preparation is automated, reducing the labour involved in utilising the selectivity of ion-selective electrodes.

References on page - 29 -

2.6 **REFERENCES:**

1. DAHMEN EAMF, *Electroanalysis: theory and applications in aqueous and non-aqueous media and in automated chemical control.* Amsterdam: Elsevier Science Publishers (1986) 383p. Techniques and instrumentation in analytical chemistry - Volume 7. ISBN 0-444-42534-9

2. Recommendations for Nomenclature of Ion-selective electrodes. *Pure and Applied Chemistry* (1975) 1-J **48**:129-132

3. BUCK Richard P, Crystalline and Pressed Powder Solid Membrane Electrodes. In COVINGTON Arthur K, *Ion-selective Electrode Methodology. Vol. 1* Boca Raton: CRC Press (1979) vol. 1 p175-250

4. ATKINS PW, *Physical Chemistry.* 6th ed. Oxford: Oxford University Press (1998) 1014p. ISBN 0-19-269068-X

5. CAMMANN K, *Working with Ion-Selective Electrodes.* Translated by AH Schroeder. 2nd ed. Berlin: Springer-Verlag (1977)) 225p. ISBN 3-540-09320-6

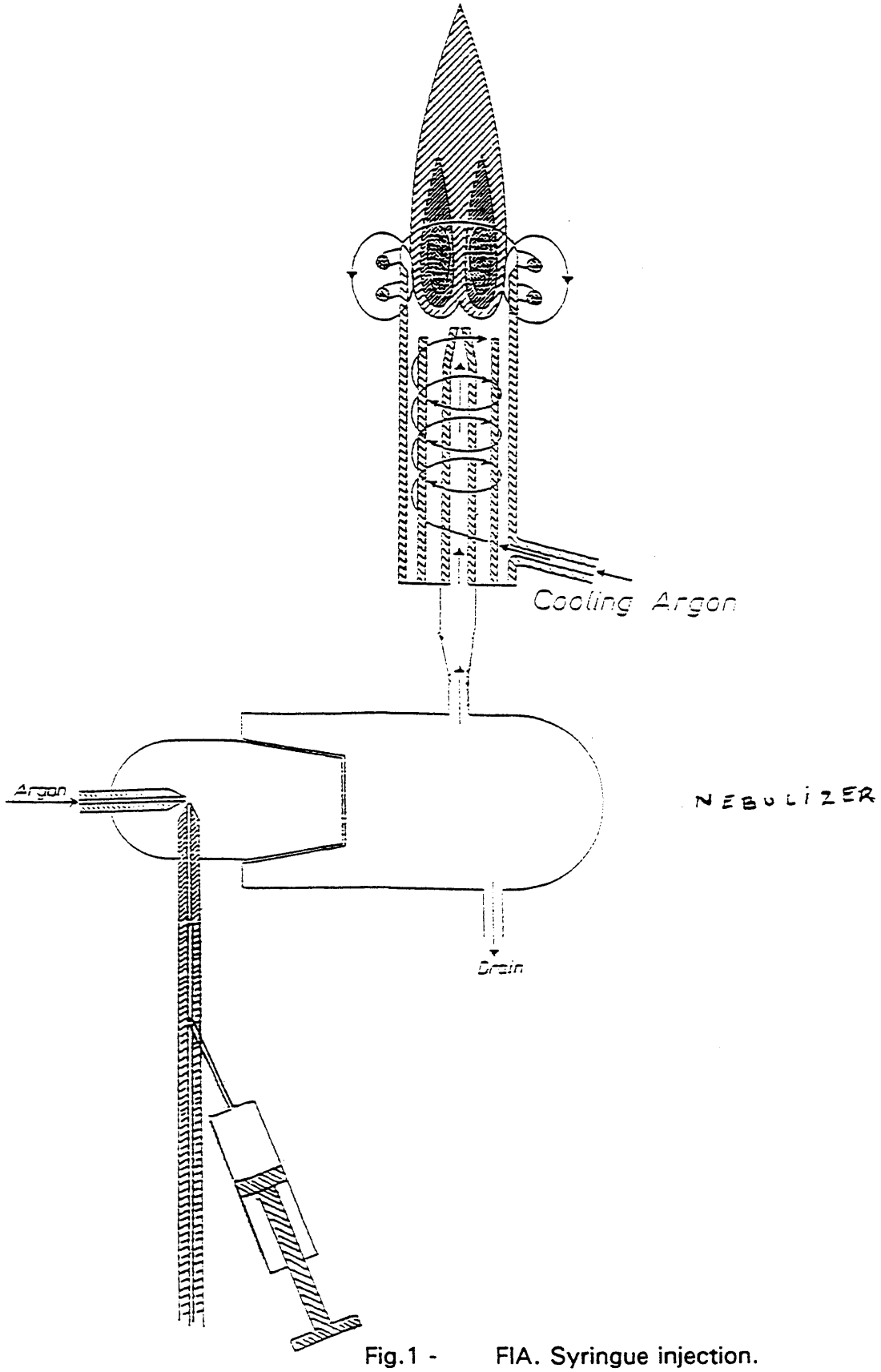

Fig.1 - FIA. Syringue injection.

Chapter 3

Simultaneous Determination of Chloride and Bromide

3.1 **INTRODUCTION**

The first report of multiple determinations by an array of ISEs was by Virtanen [1]. He used a linear model to separate the effects of sodium, potassium, calcium, and chloride on an array of their ISEs, in the concentration range encountered in human physiology.

The response function

$$y = c_r e^{\Delta E/S}$$

where c_r: analyte concentration in carrier

ΔE: peak height

S: slope of electrode

was regressed on the concentrations of the analytes using the equation

$$y = c_1 + k_2c_2 + k_3c_3 + k_{12}c_1c_2 + k_{13}c_1c_3 + k_{23}c_2c_3 + k_{123}c_1c_2c_3$$

(It is assumed that the selectivity is constant, and prior knowledge of the electrode slope is needed.) An increase in the precision of the analysis of a solution of mixed ions was reported. The correction coefficients were purely formal, and had no connection with "real" electrode selectivity coefficients. The interaction coefficients k_{ij} and k_{123} were found to be insignificant.

Otto and Thomas [2] followed, with a system using OLS (ordinary least squares) and PLS (partial least squares). The Nikolskii equation

$$E = E° + S\log(c_1 + K_{12}c_2)$$

was transformed to

$$10^{E/S} = 10^{E°/S}c_1 + 10^{E°/S}K_{12}c_2$$

Using the previously measured slope for the electrode as a constant, the transformed potential ($10^{E/S}$) was regressed on the concentrations c_1 and c_2. In this way an array was devised for the determination of magnesium, calcium, sodium and potassium at physiological concentration levels.

References on page - 59 -

Beebe *et al.* [3] extended this work by using variable slope and simplex optimisation to determine the Nikolskii-equation parameters of sodium and potassium electrodes. Once K is fixed, the problem turns linear, and is simple to solve.
The steps used for the non-linear regression (NLR) is as follows:

1. Estimate a value for K_{12} in the equation
$$E = E^\circ + S\log(c_1 + K_{12}c_2)$$

2. Set
$$L = \log(c_1 + K_{12}c_2)$$

3. Regress E on L:
$$E = E^\circ + SL$$

4. Compare the estimated potentials $\hat{E}$ with the experimental potentials E

5. Use the simplex algorithm to find a new value for K_{12}, and repeat steps 2-5 until the simplex cannot improve the estimate's accuracy.

To illustrate the idea of usefulness of low selectivity, "... it is important to note that this set of sensors would not be used by any competent analyst who suspected the presence of potassium. Individual use of the sensors is inappropriate owing to their poor selectivities. They can be used in combination with good efficiency."

Beebe and Kowalski showed [4] that predictions can be made without the Nikolskii equation, and even without an explicit model, using Projection Pursuit Regression.

This was followed by a series of papers from Dublin City University that explored the non-linear calibration of electrode arrays using iterative algorithms. No assumption was made about the slope, and E°, S, and K were all determined by an iterative algorithm

References on page - 59 -

from the calibration data. It was assumed that selectivity coefficients stay constant. At first the measurements for the calibration and analysis were equilibrium potential measurements, made in static solutions [5,6]. The same algorithms were soon successfully applied to transient potential measurements measured under the dynamic conditions of flow-injection analysis [7,8,9] and batch injection analysis [10].

All the work above used non-crystalline ISEs. In monitoring applications, where low maintenance is a desirable attribute, the use of solid-state electrodes would be ideal. In the work presented here, the methods of Diamond *et al.* [9] were applied to measurements made by solid state silver-salt based ion-selective electrodes.

References on page - 59 -

3.2 EXPERIMENTAL

3.2.1 **Instrumentation** (Figure 1)

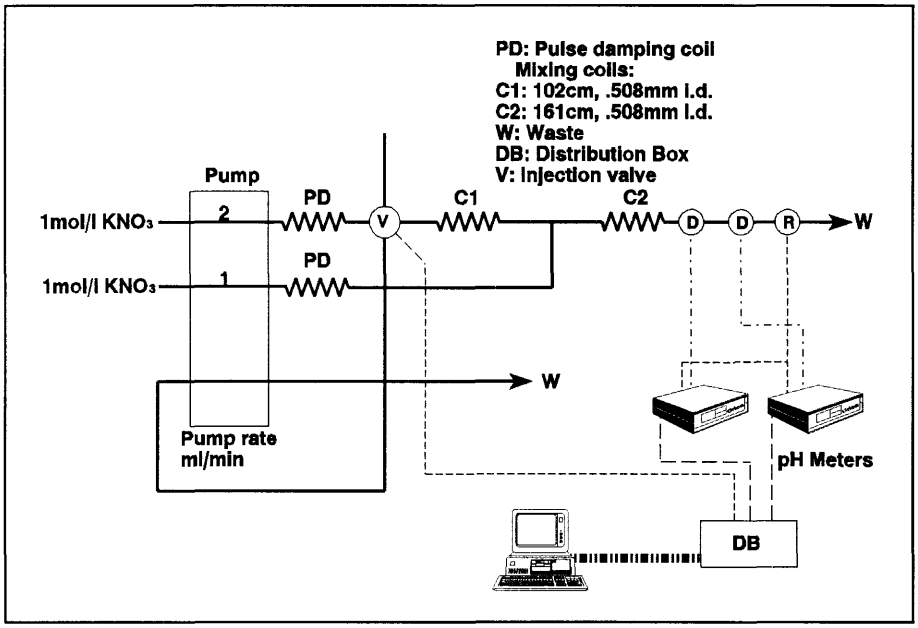

Figure 1. Schematic representation of the flow-injection system. SISTEEM.WPG

The instrumentation used in this part consisted of three subsystems:

Potentiometry subsystem

Initially solid state tubular electrodes for chloride and bromide, made in the laboratory, were used. These consist of a silver metal tube with a thin layer of silver halide deposited on the inner surface [11]. The halide layer is the ion-selective membrane, and the silver metal acts as electrical contact. Electrolyte flow is parallel to the bore of the tube and, as the electrode has tubing connectors built-in, no special holder is needed.

When the tubular electrodes were found inadequate, Orion ion-selective electrodes (Orion Research Incorporated, Boston, MA) were used.

Chloride: Model 94-17B

Bromide: Model 94-35

References on page - 59 -

Iodide: Model 95-53

An Orion Model 90-02 double junction reference electrode was used in all the potential measurements.

In the rest of this chapter the chloride, bromide, and iodide selective electrodes will be called **CL**, **BR**, and **IO**, respectively.

Potentials were measured with two Orion Research Microprocessor model 901 Ionalysers. The chart recorder binding posts of these potentiometers were connected to the analog input of the distribution box of the FlowTEK system. A full-scale readout of the Ionalyser (± 999.9 mV) gives a signal of ±100 mV at the binding posts.

Flow injection subsystem

Solutions were propelled by a 6-roller peristaltic pump running at 20 rpm. The manifold was built of Tygon tubing with an internal diameter of 0.51mm. A 10 port rotary valve from Valco Instrument Corporation (Houston, Texas, USA) was used as injection device. (Figure 2). It is electrically actuated and can be switched to either of two positions.

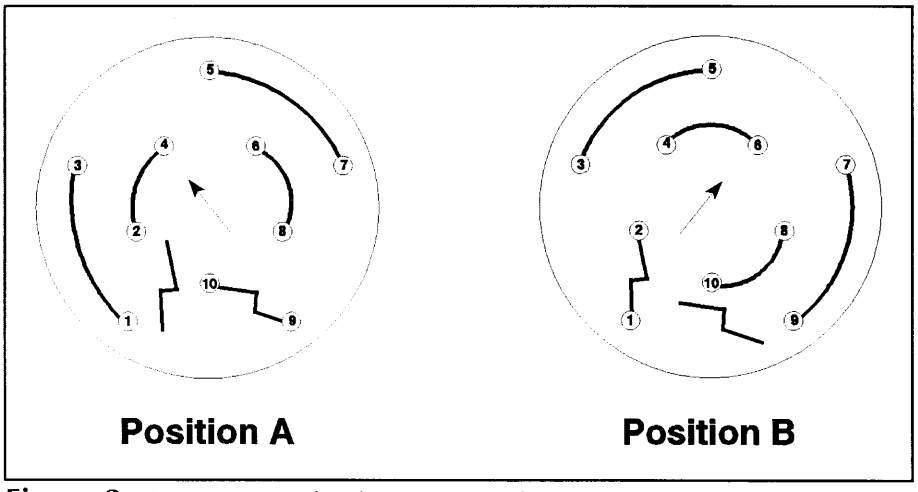

Figure 2. Connectivity of Valco 10-port valve. KLEP.WPG

A Perspex flow cell brought the electrode into contact with the flowing stream (Figure 3).

References on page - 59 -

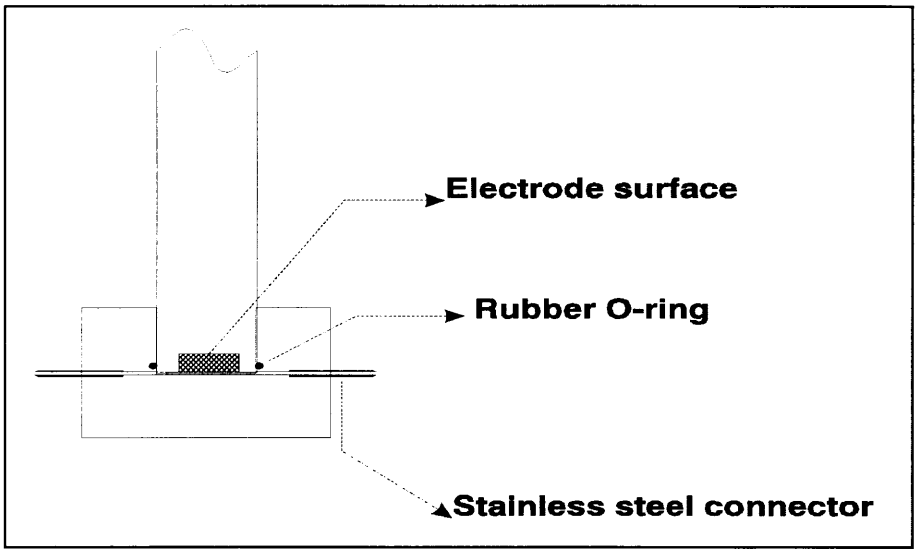

Figure 3. Construction of Flow-through cell CAP.CGM

The control & data collection subsystem

An IBM PC AT-compatible microcomputer using a 33 MHz Intel 80486 DX CPU with 4 megabyte RAM was the mainstay of the subsystem. All device control and data acquisition were done by this computer.

Devices were controlled and data collected by the FlowTEK package, supplied by Mintek (Mintek, Randburg, South Africa). The package consists of a terminal box, providing signal amplification and convenient connections, an Eagle Electronic PC-30B I/O board, and a computer program [12]. The PC-30B is a full size, low cost, high accuracy analog and digital I/O board for IBM compatible microcomputers. It features 16 analog input channels with 30 kHz throughput and 12 bit resolution, two 12 bit D/A outputs, two 8 bit D/A outputs, and 24 digital I/O lines. Advanced DMA circuitry allows multi-channel operations at full throughput. The FlowTEK package has room for expansion, for it uses only four of the analog input lines (configured for an input of 0 to +10 V), and eight of the digital output lines. Individual digital output lines can be configured, at the terminal box, for TTL (transistor-transistor logic) or switch logic operation. The Valco valve was controlled by switch logic.

References on page - 59 -

Since the binding posts gave a maximum output of 100 mV, the gain of the amplifier in the terminal box was set to 100, its maximum.

The spreadsheet package Lotus 1-2-3 Release 2.4 was used for all statistical processing and calculations. Programs to give random sample order were written in Microsoft QBasic Version 1.1.

3.2.2 **Reagents**

Carrier stream: 1 molℓ^{-1} $NaNO_3$ (extra pure, Merck)
Standards: Chloride: NaCl (AR, Associated Chemical Enterprises)
Bromide: NaBr (UNIVAR, Saarchem)

3.2.3 **Calibration**

A fully factorial, 2-factor, 5-level experiment was designed to set up the calibration equations. The samples, containing 10, 50, 250, 1000, and 5000 mgℓ^{-1} of each ion, were presented to the instrument in random order. The electrodes, individually, respond linearly in this range [13]. Since an ionic strength adjustor was used as carrier stream, ion activities were proportional to the ion concentrations, and the terms activity and concentration are used interchangeably.

A simplex method was used to find the parameters that best describe the electrode potentials in terms of concentrations. The simplex is a computational device that seeks the minium or maximum value of a function numerically. This function is often called a *response surface*, for it is an object in a multidimensional *space*.

The response surface of which the minimum was sought was the sum of squares

$$R = \sum_{i=1}^{n} (E_{ij}^{\exp} - E_{ij}^{model})^2$$

References on page - 59 -

where

$$E_{ij}^{model} = E_i^{\circ} - S_i \log(c_j - K_{jl}c_l)$$

The parameters E_i°, S_i and K_j define the space. The simplex method found the point in the space where R had a minimum value.

Appendix 2 contains a listing and explanation of the spreadsheet implementation of the simplex algorithm.

3.2.4 **Prediction**

The Nikolskii equation can be rearranged to give:

$$10^{(E_{ij} - E^{\circ}_i)/S_i} = a_{ij} + K_{jl}a_{il}$$

where $i = 1,2,...,n$, n being the number of potentials measured in mixed solutions. For two sensors this gives rise to a system of two equations, which can be represented in matrix form as

$$\mathbf{C} = \mathbf{AK}$$

where **C** is an $n \times 2$ matrix defined by the left-hand side of the rearranged Nikolskii equation, **K** is a 2×2 matrix of selectivity coefficients for the two electrodes of which the diagonal elements are unity, and **A** is a $n \times 2$ matrix of the unknown activities of the chloride and bromide ions. By inverting the matrix **K** we obtain

$$\mathbf{A} = \mathbf{CK}^{-1}$$

where $\mathbf{K}^{-1}$ is the inverse of **K**. The activities of the cations are then contained in the matrix **A**.

This procedure differs from that used by Forster and Diamond [7] in the use of $n \times 2$ matrices rather than 2×1 column matrices. In a spreadsheet vertical matrices are easier to work with than horizontal ones.

References on page - 59 -

A matrix **K** is invertible if, and only if, the system **KX** = **0** has only the trivial solution [14]. It can be shown that for some values of K_{jl} a non-trivial solution exists, and that for these values $K_{12}K_{21} = 1$. **K** is therefore only invertible if $K_{12}K_{21} \neq 1$. For selectivity coefficient matrices larger than 2×2 more conditions must be satisfied, *e.g.* **K** is invertible only if $K_{12}K_{21} \neq 1$, $K_{23} \neq K_{12}K_{31}$, etc.

References on page - 59 -

3.3 TUBULAR ELECTRODES

3.3.1 Results

Tubular chloride electrodes quickly become bromide electrodes when used in solutions containing bromide.

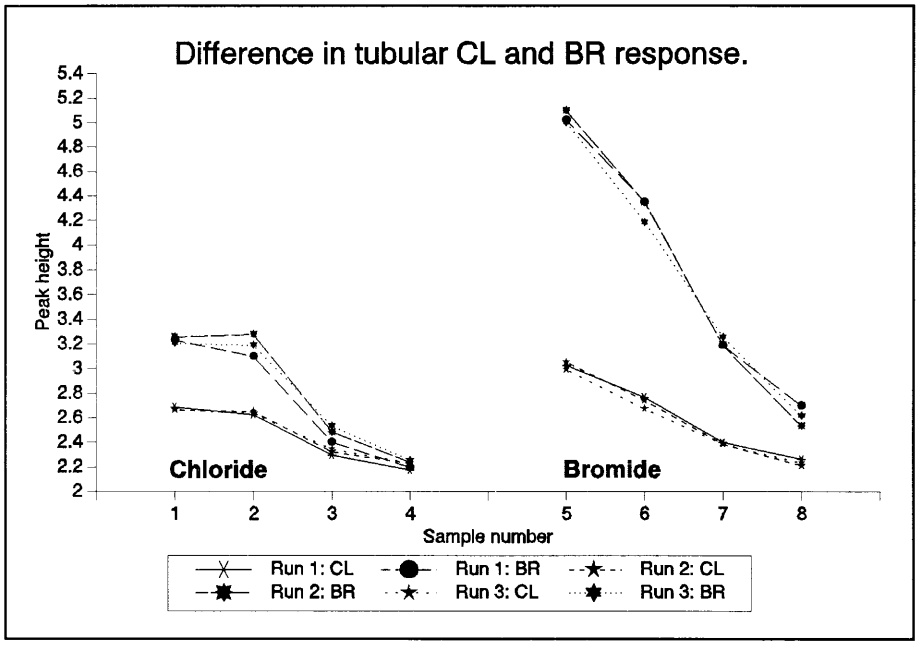

Figure 4. Difference in electrode response to separate solutions of primary ions. SEPARATE.WPG

When first used in separate solutions, the chloride and bromide selective electrodes (from here on called **CL** and **BR**, respectively) showed different responses to chloride and bromide ions in solution (Figure 4).

Soon, when used in mixed solutions of chloride and bromide, **CL** started following **BR**. Figure 5 shows a graph of the difference in peak height as recorded by **CL** and **BR** on two consecutive days. A change in the flow conditions caused a big change in sensitivity from the one day to the next.

References on page - 59 -

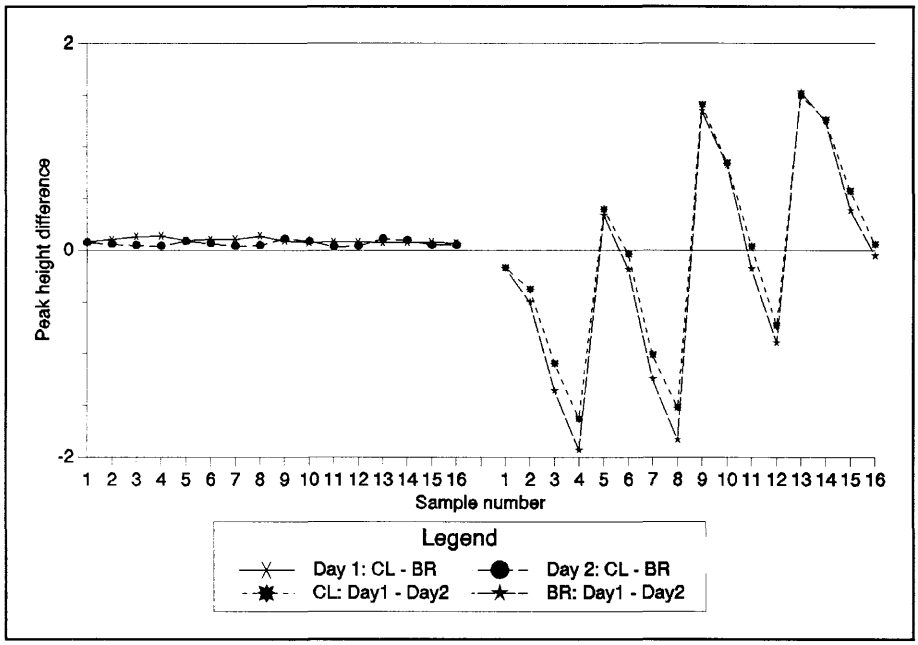

Figure 5. Difference in electrode responses to mixed samples. DIFF10.WPG

After four days, during which numerous runs of mixed solutions were made, **CL** followed **BR** exactly (Figure 6). Although the FI profiles recorded on the two consecutive days were now highly repeatable, the difference between **CL** and **BR** was less than the difference between a single electrode on two consecutive days. The small difference remaining between **CL** and **BR** peak heights can be attributed to the slightly higher dispersion for the second electrode in the array (**BR**).

3.3.2 **Discussion**

When AgCl is in contact with water, some of it will dissolve until its solubility product is reached. When it is in contact with a bromide solution AgBr will be precipitated if $a_{Br} \geq a_{Cl}\, s_{AgBr}/s_{AgCl}$, so that bromide is removed from the solution adjacent to the AgCl membrane (s_{MX} is the solubility product of the salt). The bromide is continuously resupplied from the bulk solution by diffusion and reacts with Ag^+ ions originating from the membrane. This continues until either the AgCl of the membrane or the bromide from the solution is exhausted. Under flow-injection conditions the former is the case, and the thin layer and small surface (36 mm²) of AgCl in the tubular electrode reaches

References on page - 59 -

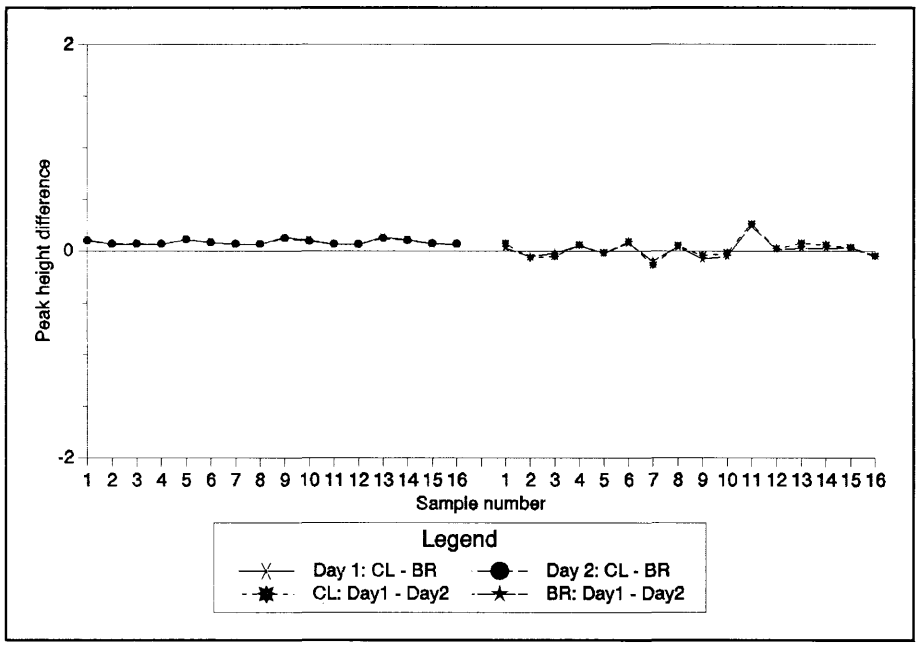

Figure 6. Difference in electrode responses: 4 days later. DIFF20.WPG

this state rapidly.

When the Nikolskii equation is used to model these identical electrodes, the expected happens: in the equation for the first electrode (**CL**) there is a very high selectivity coefficient, while the equation for **BR** has a very low selectivity coefficient:

$E_{CL} = -1.623 + 2.531 \log ([Cl] + 8.511[Br])$

$E_{BR} = 0.504 + 2.464 \log ([Br] + 0.082[Cl])$

When it was noted that the slopes were approximately equal, the first equation was rearranged to give:

$E_{CL} = 0.731 + 2.531 \log ([Br] + 0.117[Cl])$

The small difference between the selectivity coefficients in the last two equations is another indication that the electrode responses are very similar.

Because two identical electrodes cannot be used to model two species, tubular electrodes were abandoned in favour of commercially available bromide- and chloride-selective electrodes.

References on page - 59 -

3.4 CHLORIDE & BROMIDE ELECTRODES

3.4.1 Results

A pair of electrodes (Chloride and Bromide) was bought and, as a preliminary, their selectivities towards bromide and chloride (respectively) were measured using the "fixed interference" method recommended by the IUPAC [15]. The method was modified by using simulation instead of a graphical method of determine the selectivities. Six solutions were used, each containing, besides an ionic strength adjuster, 100 $mg\ell^{-1}$ interfering ion (a_j) and 0, 50, 100, 500, 1000, and 5000 $mg\ell^{-1}$ primary ion (a_i). The potential E_i of the electrode in each solution was measured. Using the spreadsheet, the potential was regressed on the expression $\log(a_i + k_{ij}a_j)$. The value of k_{ij} was adjusted manually until the correlation coefficient (r^2) achieved a maximum value. A small macro was used to automate this procedure. This approach is in effect the same as the one used by Beebe *et al.* [3], but uses a manual search of the single parameter, instead of an automated simplex search.

The following expressions were derived in this manner:

CL	$E = 241.8 - 54.22 \log ([Cl] + 0.65771\ [Br])$	$r^2 = 0.999509$
BR	$E = 116.4 - 58.79 \log ([Br] + 0.006952\ [Cl])$	$r^2 = 0.999986$

The slopes in these cases are Nernstian, and the selectivity coefficients comparable to those obtained by others [16,20].

These good results lead one to believe that the electrodes can be used in an array.

When these electrodes were used as an array detector in FIA, however, the results were disappointing:

References on page - 59 -

The fitted equations are:

CL $E = 0.4979 + 0.2876 \log ([Cl] + 0.6310\,[Br])$ $R^2 = 0.949972$

BR $E = 0.5735 + 0.4202 \log ([Br] + 0.0109\,[Cl])$ $R^2 = 0.979562$

(Note that the slopes and intercepts of these equations cannot be directly compared with those of the previous equations. The first set was generated by taking the mV readings directly from the pH meter under static conditions. The second (array) set was generated from the peak heights reported by FlowTEK. These were measured under FIA conditions, amplified and inverted to give a 0-10 V signal proportional to the potential of the electrode.)

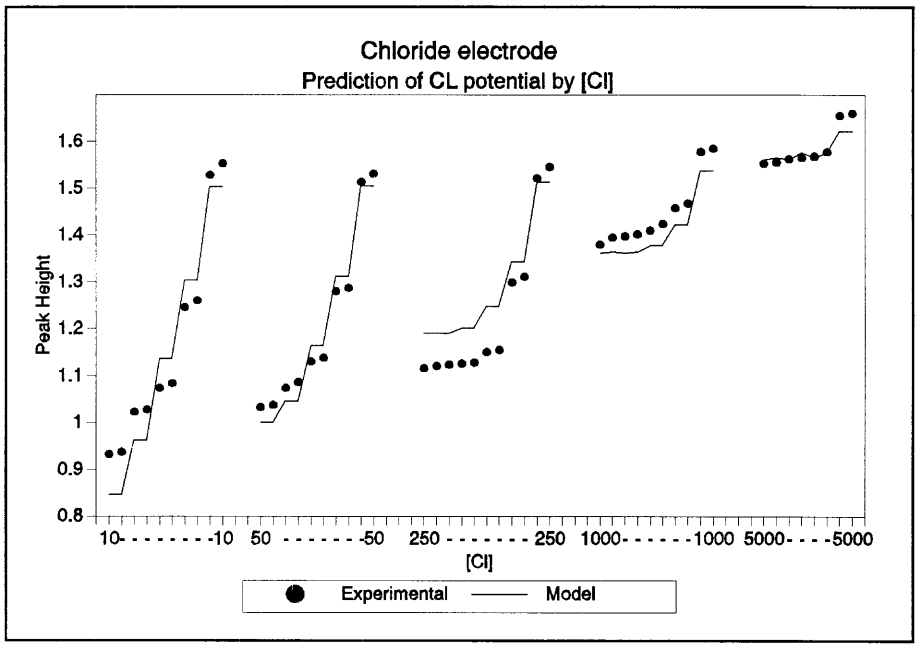

Figure 7. Prediction of chloride electrode response. 20RESPCL.WPG

As shown in Figure 7 and Figure 8, the prediction of potentials only holds at high primary ion/interfering ion ratios. The overall form of the prediction is good, but it shows significant structure in the residuals at low primary ion concentrations.

When these models are used to predict the concentrations of samples, the predictions, as can be expected, are widely scattered. The amount of scatter is shown in the scatterplots Figure 9 and Figure 10. In some cases negative concentrations were

References on page - 59 -

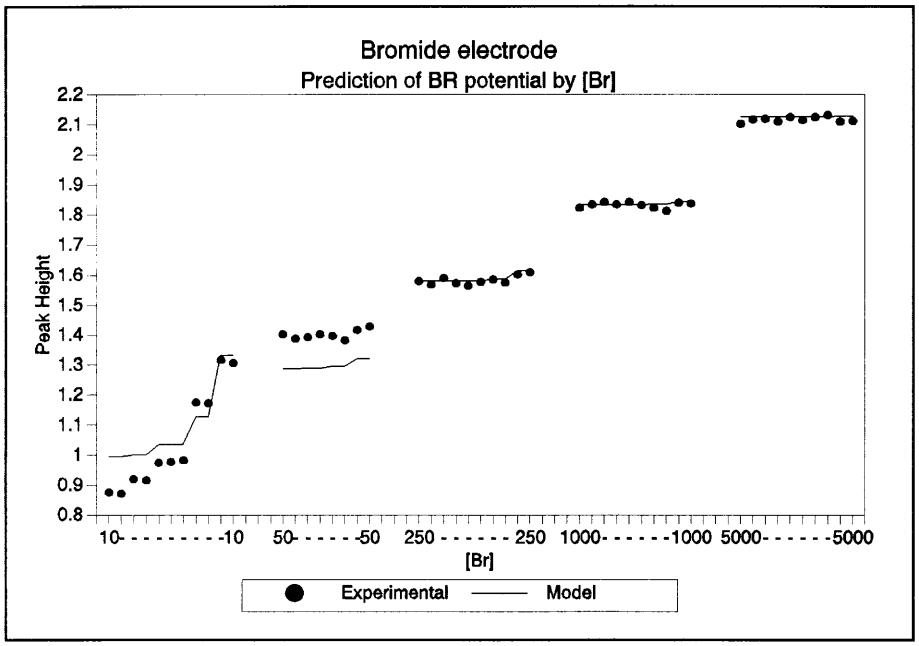

Figure 8. Prediction of bromide electrode response. 20RESPBR.WPG

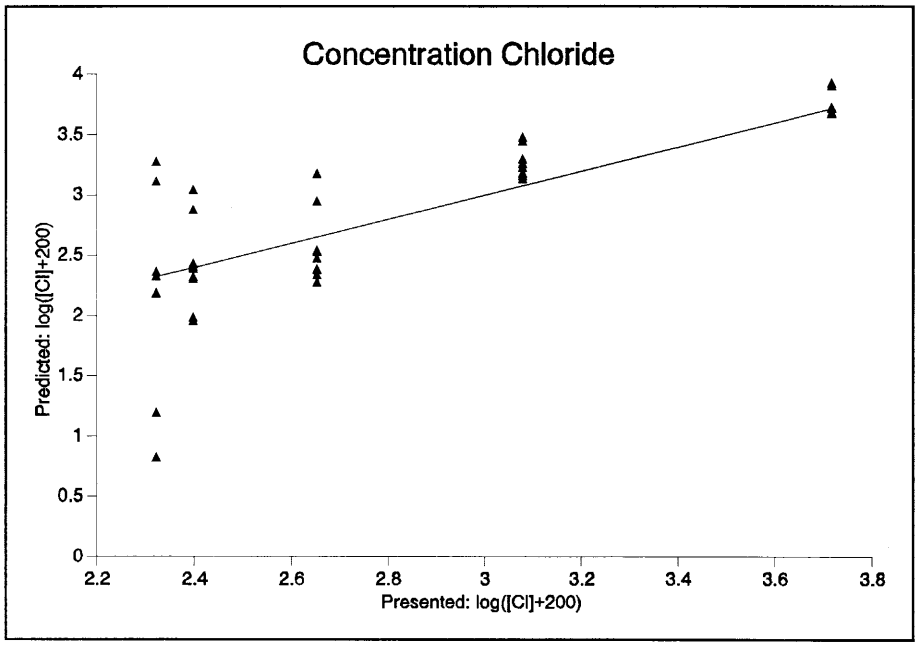

Figure 9. Scatterplot of chloride concentration prediction. 20SCATCL.WPG

predicted, so that in Figure 9 a constant had to be added to the concentration to show it on the log-log axes.

References on page - 59 -

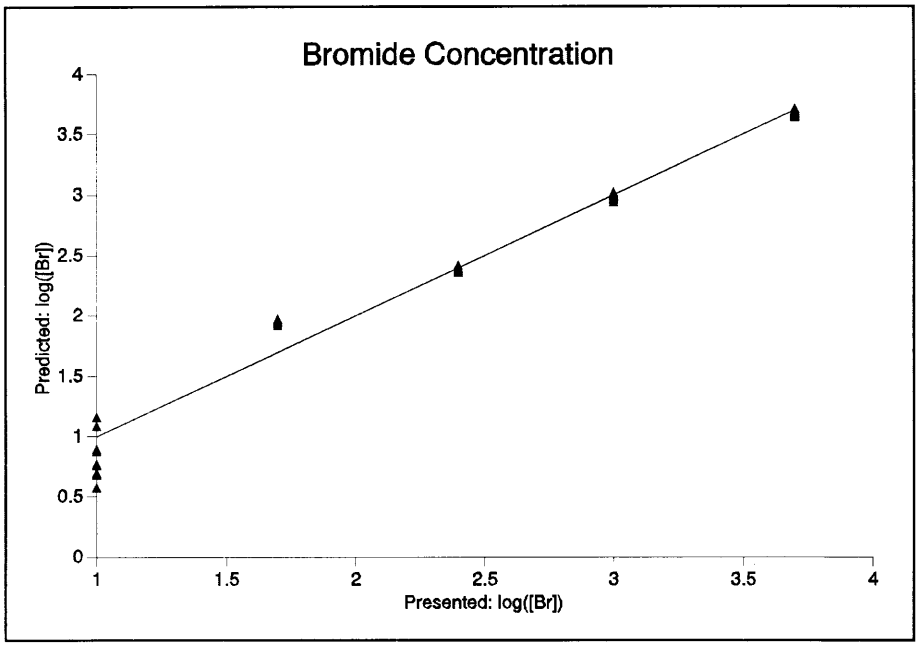

Figure 10. Scatterplot of bromide concentration prediction. 20SCATBR.WPG

3.4.2 **Discussion**

To isolate and evaluate all the errors involved it is necessary to do a comprehensive error analysis. "The most widely used method of estimating the variance of a statistic that is a function of several variables is to expand the statistic into a Taylor series, drop all but the first order terms and use the rules for the linear combination of variables to estimate the variance. That is known as *propagation of error* or the *delta method.*" [17] The procedure given by Clifford [18] for propagating errors from *n* variables to *n* statistics was used.

To propagate the error two things are needed:

1. An estimate of the variance of the variables used to calculate the statistic.
2. A set of derivatives of the equations that connect the statistics to the variables.

   In the case where equations are not available a derivative must be found numerically.

References on page - 59 -

Estimating the Variance

As the two replicates in the data set of Figure 7 and Figure 8 were not enough to get a good estimate of the variance, data from an experiment in repeatability was used. Four injections were made of each of three standard solutions, each containing both ions at one of three levels: 5000, 1000 or 500 $mg\ell^{-1}$.

From the peak heights of these injections the variance-covariance matrix $\mathbf{M}_E$ was calculated.

$$\mathbf{M}_E = \frac{1}{N}\sum_{i=1}^{N} \boldsymbol{\delta}\mathbf{E}_i \boldsymbol{\delta}\mathbf{E}_i^T$$

where $\boldsymbol{\delta}\mathbf{E}_i$ is the deviation from the average of the *i*th set of four observations. The following table summarises the three variance-covariance matrices:

$[Cl^-]/mg\ell^{-1}$	$[Br^-]/mg\ell^{-1}$	var(**CL**)[1]	var(**BR**)[1]	cov(**CL**,**BR**)[1]	corr(**CL**,**BR**)[1]
5000	5000	0.000637	0.000185	0.000290	0.845
1000	1000	0.000405	0.000946	0.000534	0.863
500	500	0.000220	0.000121	0.000131	0.804
	Average:	0.000421	0.000417	0.000319	0.761

The high correlation between the errors is to be expected. Since the variations in the peak height depends on both variation in the flow domain and variation in the electrode domain, and variation in the flow domain is common to both electrodes, the covariance cannot be zero.

For calculation, the averages of the variances and covariances were used.

Finding the Derivatives

The Nikolskii equations used in the model of the electrodes are:

[1] The *variance* (var(x) or σ_x^2) is a measure of the error in a quantity x. The *covariance* cov(x,y) is a measure of how much the errors in two quantities are correlated. The *correlation coefficient* (corr(x,y) or $\rho_{x,y}$) is defined as cov(x,y)/(var(x)·var(y)), and is a normalized, unitless indicator of the strength of the correlation.

References on page - 59 -

$$E_{CL} = E_{CL}^{\circ} + S_{CL} \log([Cl] + K_{CL}[Br])$$

$$E_{BR} = E_{BR}^{\circ} + S_{BR} \log(K_{BR}[Cl] + [Br])$$

Using matrix notation:

The concentrations **C** is a function of the potentials **E**

$$\mathbf{C} \equiv \mathbf{C}(\mathbf{E})$$

where **E** and **C** are column matrices:

$$\mathbf{E} = \begin{bmatrix} E_{CL} \\ E_{BR} \end{bmatrix} \quad \text{and} \quad \mathbf{C} = \begin{bmatrix} [Cl] \\ [Br] \end{bmatrix}$$

The approximation that the functions are linear in the region of the errors was verified numerically, so that $\delta\mathbf{C} = \mathbf{B}\,\delta\mathbf{E}$ where

$$\mathbf{B} = \begin{bmatrix} \dfrac{\partial[Cl]}{\partial E_{CL}} & \dfrac{\partial[Cl]}{\partial E_{BR}} \\ \dfrac{\partial[Br]}{\partial E_{CL}} & \dfrac{\partial[Br]}{\partial E_{BR}} \end{bmatrix}$$

Since

$$[Cl] = 10^{(E_{CL} - E_{CL}^{\circ})/S_{CL}} - K_{CL}[Br]$$

and

$$[Br] = 10^{(E_{BR} - E_{BR}^{\circ})/S_{BR}} - K_{BR}[Cl]$$

$$\mathbf{B} = \begin{bmatrix} \dfrac{\ln 10}{S_{CL}(1 - K_{CL}K_{BR})} 10^{(E_{CL} - E_{CL}^{\circ})/S_{CL}} & \dfrac{-K_{CL}\ln 10}{(1 - K_{CL}K_{BR})} 10^{(E_{BR} - E_{BR}^{\circ})/S_{BR}} \\ \dfrac{-K_{BR}\ln 10}{(1 - K_{CL}K_{BR})} 10^{(E_{CL} - E_{CL}^{\circ})/S_{CL}} & \dfrac{\ln 10}{S_{BR}(1 - K_{CL}K_{BR})} 10^{E_{BR} - E_{BR}^{\circ})/S_{BR}} \end{bmatrix}$$

References on page - 59 -

These partial derivatives are complex, and become more complex as the number of equations increases. For large arrays it will be simpler to obtain the derivatives numerically.

Propagating the Error

If the variance-covariance matrix of the potentials is defined as

$$\mathbf{M}_E = \begin{bmatrix} \text{var}(E_{CL}) & \text{cov}(E_{CL},E_{BR}) \\ \text{cov}(E_{BR},E_{CL}) & \text{var}(E_{BR}) \end{bmatrix}$$

then the variance-covariance matrix of the concentrations is given by

$$\mathbf{M}_C = \mathbf{B}\,\mathbf{M}_E\,\mathbf{B}^T$$

The relative errors as expected from the error propagation and the obtained relative errors are shown in Figure 11 and Figure 12. These figures echo the scatterplots: only predictions of concentrations at high primary/interfering ion rations are accurate. The greatest error is in the Cl^- standards where $[Br^-] = 5000$, but these are also the only points consistently inside the 99.7% confidence interval. The experiments are obviously biased.

The only instance where the experimental data can be thought to fit the model is for **BR** in samples which are 500, 1000 and 5000 $mg\ell^{-1}$ in Br^-. Here the measured points fall inside the confidence interval limits, and randomly around the zero-error line.

The selectivities of the electrodes are not constant enough to be of use in the Nikolskii model of an electrode array

References on page - 59 -

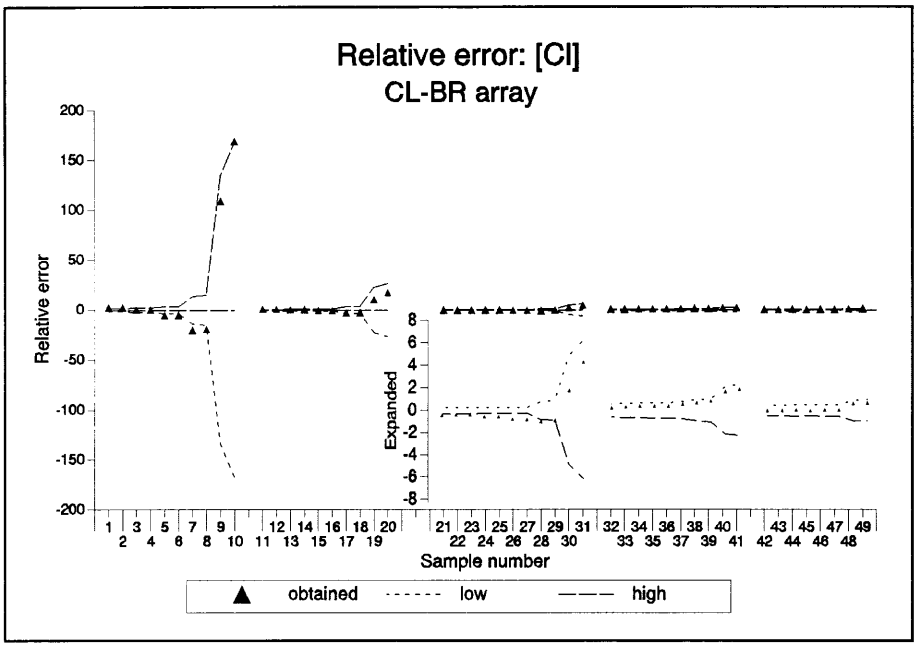

Figure 11. The expected and obtained relative errors in predicting [Cl^-]

20SCLREL.WPG

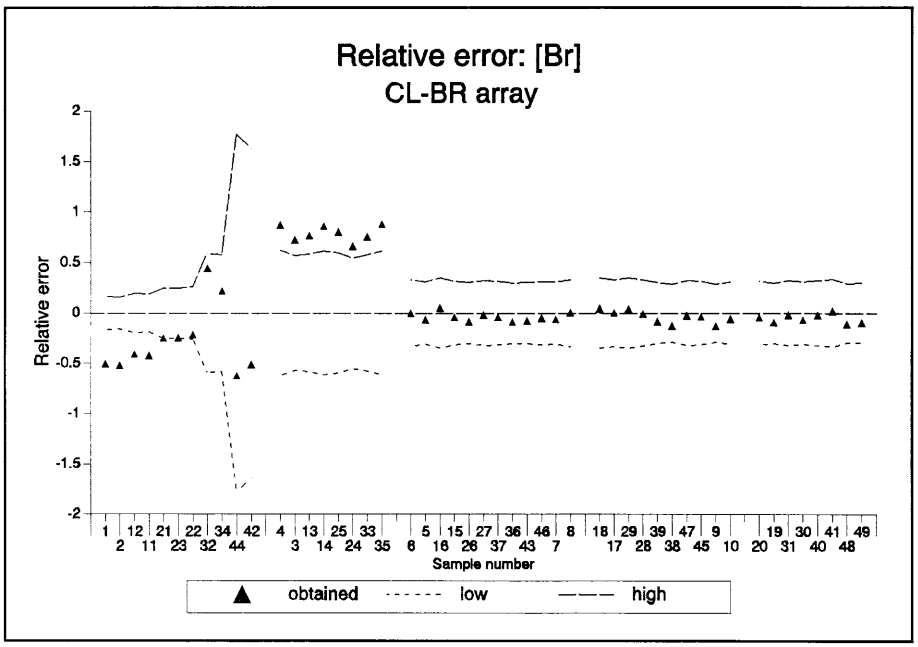

Figure 12. The expected and obtained relative errors in predicting [Br^-]

20SBRREL.WPG

References on page - 59 -

3.5 BROMIDE & IODIDE ELECTRODES

3.5.1 Results

The variation in the selectivity of the chloride electrode is presumably caused by the lower solubility of AgBr, compared to AgCl. When bromide is present in the sample, bromide reacts with silver from the membrane to precipitate AgBr on the membrane surface, changing its composition and thereby its selectivity. To avoid this it seemed possible to use a bromide electrode as a chloride detector, and an iodide electrode as a bromide detector. In this way, the solubility of the silver halides determined is always lower than the solubility of the silver salts that make up the electrodes, and the selectivity should stay constant.

When judged by the correlation coefficients the model fits better to the bromide (**BR**) and iodide (**IO**) electrode potentials than to the **CL** and **BR** potentials.

BR	$E = -0.6023 + 0.4582 \log ([Cl] + 40.6444\ [Br])$	$R^2 = 0.970641$
IO	$E = 0.2918 + 0.2856 \log ([Br] + 0.008644\ [Cl])$	$R^2 = 0.980223$

The response given by **BR** and its fit to the model are shown in Figure 13, and the same for **IO** in Figure 14. These figures also show that the fit of the model to the data seems better for the **BR-IO** array than for the **CL-BR** array.

However, when the data used to draw these graphs were used to predict the concentrations, the results were poor: errors of the magnitude of thousands of percent were obtained. A scatterplot like Figure 9 or Figure 10 shows only gibberish. Linear regression on the data of an ideal scatterplot gives an intercept of zero, a slope of one and a correlation coefficient of one. Linear regression of predicted Cl^- concentration on actual concentration predicts an intercept of -7186.17, a slope of -2.62076 and a correlation coefficient of .019274. For $[Br^-]$ the values are slightly better: intercept: -122.453, slope: 1.291038, correlation coefficient: 0.928678

References on page - 59 -

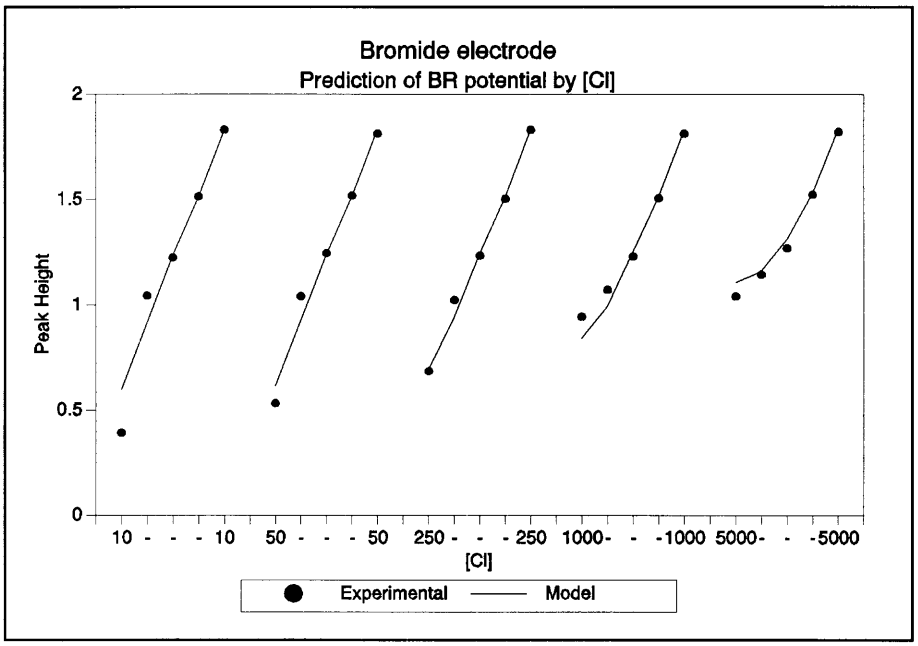

Figure 13. Prediction of bromide electrode response chloride concentration.

10RESPBR.WPG

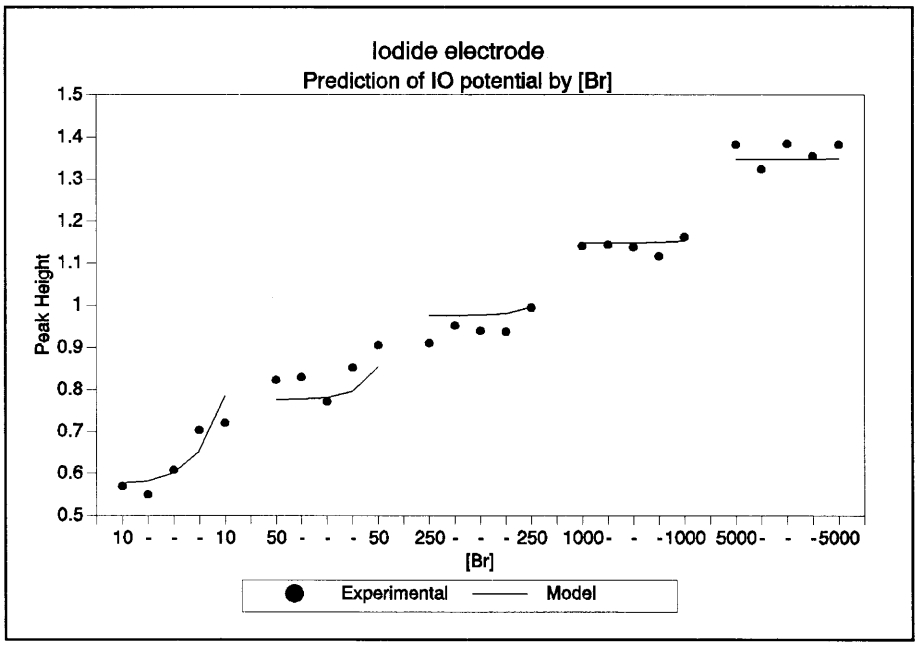

Figure 14. Prediction of iodide electrode response by bromide concentration.

10RESPIO.WPG

References on page - 59 -

3.5.2 **Discussion**

When confronted with errors of the magnitude reported in Paragraph 3.5.1 for the prediction of chloride and bromide concentrations one looks for calculation errors, but it soon proves that the calculation is in order, and that the error is an intrinsic part of the way the error is propagated. Error propagation shows that the **BR-IO** array produces a better fit to the model than the **CL-BR** array.

For the values shown in Figure 13 and Figure 14 no replicate values were taken, which means that no variances or covariances could be estimated. For error analysis an estimate of at least the variances is needed. It can be assumed that the variances of the **CL** and **BR** responses are similar to the **BR** and **IO** responses. It will also be assumed, though patently invalidly, that the covariances are negligible.

This assumed variance-covariance matrix for the potentials is then

$$\mathbf{M}_E = \begin{bmatrix} 4.2\times10^{-4} & 0 \\ 0 & 4.2\times10^{-4} \end{bmatrix}$$

and the same steps as in 3.4.2 can be followed to propagate the errors in the potentials to the expected errors in concentrations.

The expected error for [Cl] (Figure 15) and [Br] (Figure 16) are defined as three times the standard deviation. If the residuals have a normal distribution, the probability that the errors will fall in this range is 99.7%. As can be seen in the Figures, the measured error falls within this range, which means that there is no statistical reason to regard the expected concentrations as different from the obtained concentrations, although there is still some structure in the residuals. The error propagation properties of the method make the predictions useless. A relative error of 0.1 (10%) is usually considered as the lower limit of acceptable accuracy. While the model of electrode potentials meets this criterium, these errors go on to generate extremely large errors in concentrations.

References on page - 59 -

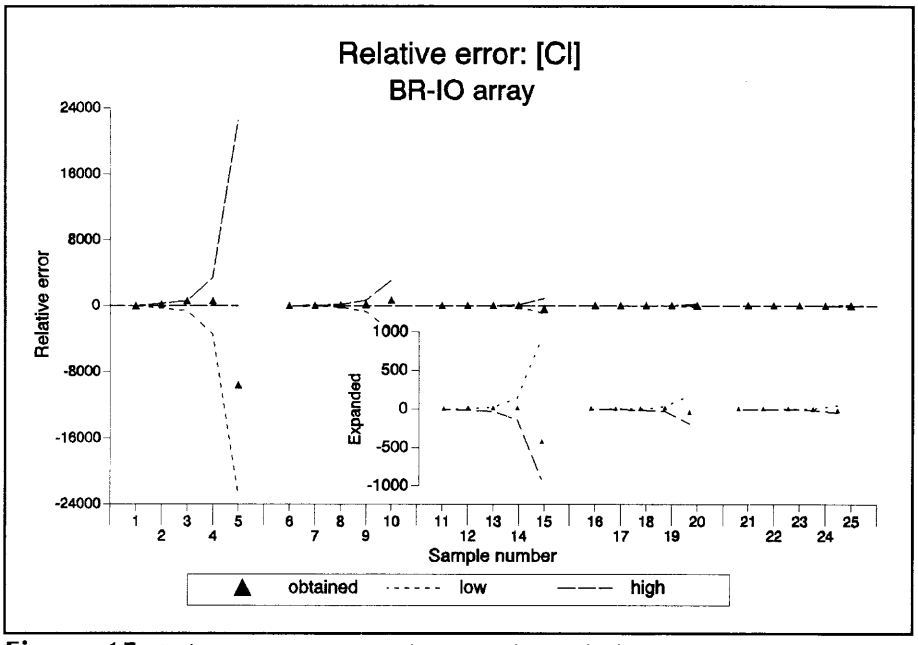

Figure 15. Relative errors in predicting [Cl^-] with the **BR-IO** array.

10NCLREL.WPG

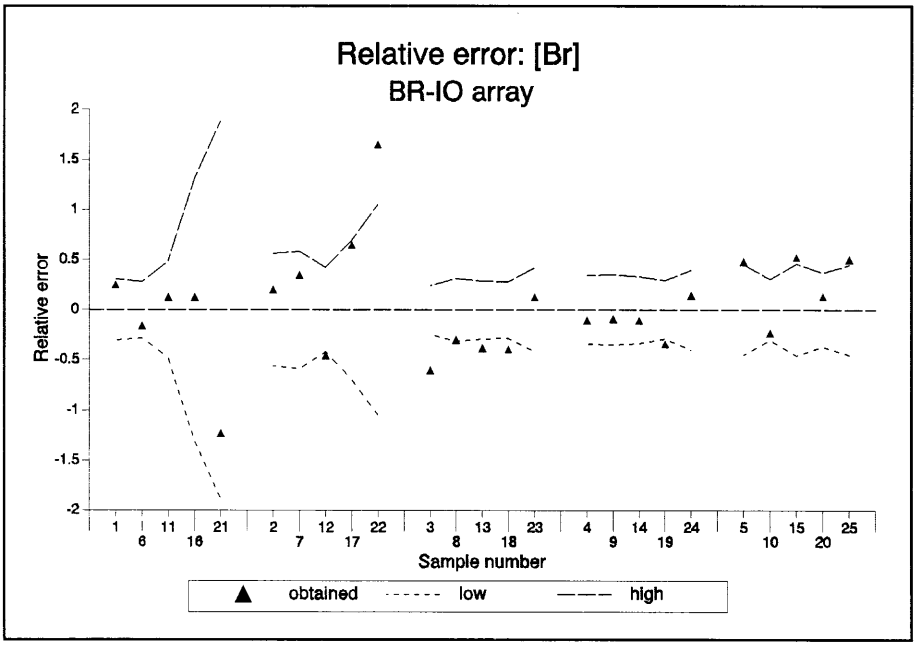

Figure 16. Relative errors in predicting [Br^-] using a **BR-IO** array. 10NBRREL.WPG

To illustrate that the problem is not one that can be solved by increasing the accuracy of measurement, consider the following: the most accurate measurement FlowTEK can make is $10V/2^{12} = 0.00244$ V. If this is considered the standard deviation of the potential measurement, and the potential measurements fit the model exactly, then the expected standard deviation of the concentration will be:

References on page - 59 -

[Cl]	[Br]	std(Cl)	std(Br)	%Cl	%Br
1000	10	26.698	2.311	2.669	23.119
1000	50	57.658	6.035	5.765	12.070
1000	250	212.456	24.352	21.245	9.741
1000	1000	792.952	92.934	79.295	9.295
1000	5000	3888.926	458.660	388.892	9.173
5000	10	102.531	7.648	2.050	76.480
5000	50	133.491	11.559	2.669	23.119
5000	250	288.290	30.175	5.765	12.070
5000	1000	868.786	98.895	17.375	9.889
5000	5000	3964.76	464.67	79.295	9.293

[Cl]	[Br]	std(Cl)	std(Br)	%Cl	%Br
10	10	7.929	0.929	79.295	9.293
10	50	38.889	4.586	388.892	9.173
10	250	193.688	22.872	1936.88	9.149
10	1000	774.183	91.446	7741.83	9.144
10	5000	3870.157	457.170	38701.57	9.143
50	10	8.687	0.988	17.375	9.889
50	50	39.647	4.646	79.295	9.293
50	250	194.446	22.933	388.892	9.173
50	1000	774.941	91.506	1549.883	9.150
50	5000	3870.915	457.230	7741.83	9.144
250	10	12.479	1.278	4.991	12.782
250	50	43.439	4.944	17.375	9.889
250	250	198.238	23.233	79.295	9.293
250	1000	778.733	91.807	311.493	9.180
250	5000	3874.707	457.531	1549.883	9.150

As can be seen from this table, the error expected is smaller for bromide than for chloride, although the error in the **BR** and **IO** potentials are equal.

The accuracy of the bromide determination exceeds the 10% limit when the ratio [Cl]:[Br] is greater than 45. This is a loss of performance, since the bromide electrode's instruction manual [13] states that (using a single electrode) accurate measurements can be made in solutions with chloride/bromide ratios of up to 300.

The **BR-IO** array fails to improve on the prediction of concentration of the **CL-BR** array, not because the model predicts the potentials less accurately, but because the error propagation properties of the method amplify the error in potential prediction into much larger errors in concentration prediction.

Electrode arrays can play a great role in separating the effects of interfering species on their ISEs. However, high selectivity is still important in reducing the magnitude of the propagated errors. Increased selectivity decreases the expected variance: the smaller the selectivity coefficients are, the closer the selectivity matrix is to an identity matrix, and the smaller the propagated errors in concentration will be. In the **BR-IO** array **IO** is more selective towards Br^- than **BR** is to Cl^-, and the expected error in bromide concentration

References on page - 59 -

is correspondingly smaller than the expected error in chloride concentration. Also, the closer the product of K_{CL} and K_{BR} is to 1, the larger the variance will be.

The higher the sensitivity of the system, the smaller the error will be. In the case of the system used for this work, the sensitivity of the electrodes are probably not as great a problem as the high dispersion of the manifold. Electrode sensitivity is constant at 59 mV per 10-fold increase in analyte concentration. Therefore, if one wants to increase the sensitivity, it will be necessary to decrease the system dispersion. As usual the sensitivity of the system has an important influence on the accuracy of measurement, but here it is especially important.

References on page - 59 -

3.6 CONCLUSION

Tubular thin-layer chloride electrodes are not suitable for array detectors involved in detecting ions that form precipitates with silver that have lower solubilities than silver chloride.

Chloride and bromide electrodes can be used in getting a rough estimate of concentrations, but the model that predicts the potentials fit the experimental data poorly. Under the conditions used, the selectivity coefficients of the chloride and bromide electrodes vary too much to be of use as parameters in a model of electrode response [19,20].

Bromide and iodide electrodes give a system that will predict potentials fairly well, but concentrations very poorly. This is a result of the error propagation properties of the calibration method, which amplifies the lack of fit between the modelled and the experimental potentials.

Two comments by Covington [21] need repeating here:

- "... for the selectivity coefficient is only an approximate quantity and varies with the concentration of interfering ion and that of background electrolyte, if any."

- "In spite of these considerations, [the equation $E = const + \log(c_1 + kc_2)$] is best regarded as an empirical equation."

The truth is that, although selectivities can be used in multivariate calibration, a theory of crystalline ISE interference that can be used as a basis for analytical methods does not exist. Furthermore, such a theory, when developed, will not necessarily apply to the dynamic conditions found in FIA.

References on page - 59 -

What this work did achieve, was to show that numerical solutions for complex problems do not need any special skill, or special tools, to apply. Numerical tools are continuously developed, and they are becoming increasingly accessible [22]. Simultaneous calibration is difficult to visualize, and people trained in classical "straight line" calibration find it difficult to use. Using a spreadsheet to process data from flow injection systems allows one to get a good grasp of the problem, and I recommend it to anyone that feels he does not understand a problem completely.

This work had some flaws:
Calibrations were done in mg/ℓ, which introduces problems of weighing when processing data statistically. These problems were largely ignored.

The system's sensitivity was too low. This can be improved by:

- using a single line manifold.
- using a properly designed flow cell.
- using greater amplification when transmitting the signal to the computer system.

References on page - 59 -

3.7 **REFERENCES**

1. VIRTANEN Rauno, A Flow Injection Analyzer with Multiple ISE-Detector. *ion-selective electrodes 3* (1981)

2. OTTO Matthias and THOMAS JDR, Model Studies on Multiple Channel Analysis of Free Magnesium, Calcium, Sodium, and Potassium at Physiological Concentration Levels with Ion-Selective electrodes. *Analytical Chemistry* (November 1985) 13 **57**:2647-2651

3. BEEBE Kenneth, UERZ David, SANDIFER James and KOWALSKI Bruce, Sparingly Selective Ion-Selective Electrode Arrays for Multicomponent Analysis. *Analytical Chemistry* (1 January 1988) 1 **60**:66-71

4. BEEBE Kenneth R and KOWALSKI Bruce R, Nonlinear Calibration Using Projection Pursuit Regression: Application to an Array of Ion-Selective Electrodes. *Analytical Chemistry* (15 October 1988) 20 **60**:2273-2278

5. FORSTER Robert J, REGAN Francis and DIAMOND Dermot, Modelling of Potentiometric Electrode Arrays for Multicomponent Analysis. *Analytical Chemistry* (1 May 1991) 9 **63**:876-882

6. FORSTER Robert J and DIAMOND Dermot, Multivariate Calibration of Potentiometric Sensor Arrays. *Analytical Proceedings* (April 1991) **28**:117-122

7. FORSTER Robert J and DIAMOND Dermot, Nonlinear Calibration of Ion-Selective Electrode Arrays for Flow Injection Analysis. *Analytical Chemistry* (1 August 1992) 15 **64**:1721-1728

8. DIAMOND Dermot and FORSTER Robert J, Robust estimation of selectivity coefficients using multivariate calibration of ion-selective electrode arrays. *Analytica Chimica Acta* (1993) 1 **276**:75-86

9. SÂEZ DE VITERI FJ and DIAMOND Dermot, Determination and Application of Ion-Selective Electrode Model Parameters Using Flow Injection and Simplex Optimization. *The Analyst* (May 1994) 5 **119**:749-758

10. DIAMOND Dermot, LU Jianmin, CHEN Qiang and WANG Joseph, Multicomponent batch-injection analysis using an array of ion-selective electrodes. *Analytica Chimica Acta* (1993) 3 **281**:629-635

11. VAN STADEN Jacobus F, Flow injection Determination of Inorganic Bromide in Soils with a Coated Tubular Solid-state Bromide-selective Electrode. *Analyst* (May 1986) 5 **112**:595-599

12. MARSHALL GD and VAN STADEN JF, Computer-Aided Flow-Analysis for Laboratory use and Process Analysis. *Analytical Instrumentation* (1992) 1 **20**:79-100

13. *Model 94-35 and 94-53 Halide Electrodes: Instruction Manual.* Orion Research Incorporated. (1991) 37p.

14. ANTON Howard, *Elementary Linear Algebra.* 5th ed. New York. John Wiley (1987) 475p. ISBN 0-471-84819-0

15. Recommendations for Nomenclature of Ion-selective electrodes. *Pure and Applied Chemistry* (1975) 1-J **48**:129-132

16. UMESAWA Yoshio (Ed.), *CRC Handbook of Ion-Selective Electrodes: Selectivity Coefficients* Boca Raton: CRC Press (1990) 848p. ISBN 0-8493-0546-2

17. TIETJEN Gary L, *A topical dictionary of statistics* New York: Chapman and Hall (1986) ISBN 0-412-01201-4

18. CLIFFORD AA, *Multivariate error analysis: A handbook of error propagation and calculation in many-parameter systems.* London: Applied Science Publishers (1973) 112p. ISBN 0-85334-566-X

19. KLASENS HA and GOOSSEN J, The iodide interference with silver chloride electrodes. *Analytica Chimica Acta* (1977) **88**:41-46

20. HULANICKI Adam and LEWENSTAM Andrzej, Interpretation of selectivity coefficients of solid-state ion-selective electrodes by means of the diffusion-layer model. *Talanta* (March 1977) **24**:171-175

21. COVINGTON AK, Introduction: Basic Electrode Types, Classification, and Selectivity Considerations. In COVINGTON Arthur K, *Ion-selective Electrode Methodology*. Boca Raton: CRC Press (1979) vol. 1 p1-20

22. WALSH S and DIAMOND D, Non-linear curve fitting using Microsoft Excel *solver*. *Talanta* (April 1995) 4 **42**:561-572

Chapter 4

The Simultaneous Use of Chloride and Fluoride Ion-selective Electrodes in a Flow-injection Manifold.

4.1 INTRODUCTION

Fluoride is recognised as an important factor in dental health. As first identified in the USA during the 1930's, an excess of fluoride in drinking water causes fluorosis [1]. Fluorosis is a changed state of tooth enamel, and its severity depends on the quantity of fluoride ingested: at low level mottling of the teeth is visible, at higher levels they appear stained, and in extreme cases the teeth loose mechanical strength and erode rapidly.

More than 1.5 $mg\ell^{-1}$ of fluoride in water is considered harmful.

The other aspect of fluoride's impact on dental health is that an inadequate amount of fluoride in the diet leads to a higher incidence of dental caries. Dental caries is a common disease, and costs millions to combat medically.

Less than 0.5 $mg\ell^{-1}$ fluoride in water is considered inadequate [2].

Beyond dental health, fluoride at low levels is also important in the forming of a solid skeleton, while excess fluoride causes skeletal fluorosis, characterised by excessive bone growth and calcification of connective tissue.

Because fluoride is so important, public water is sometimes fluoridated. In South Africa water is not fluoridated because the recirculation of water may lead to fluoride building up to dangerous levels. If South African water is ever to be fluoridated, its concentration will have to be monitored.

Different from fluoride, chloride has no health implications. At more than 250 $mg\ell^{-1}$ Cl^- water acquires a salty taste, but only with continuous use of water with 1000 $mg\ell^{-1}$ Cl^- does kidney disease appear [2]. Natural waters with such concentrations of chloride are not common.

References on page - 91 -

The necessity of monitoring chloride has another origin: chloride is an indicator of pollution. The concentration of chloride in natural, unpolluted water, even if it is high, is constant over time. If the chloride concentration suddenly rises, it is an indicator that the water is being polluted [2].

Concrete, cement, and steel are corroded by high concentrations of chloride. Steel pipelines and concrete reinforcing are examples of areas where corrosion is a particular problem.

This project investigates the requirements of analysers that make use of simultaneous determination of fluoride and chloride with an array of ion-selective electrodes to monitor the level of these two anions in water.

References on page - 91 -

4.2 EXPERIMENTAL

4.2.1 **Instrumentation** (Figure 1)

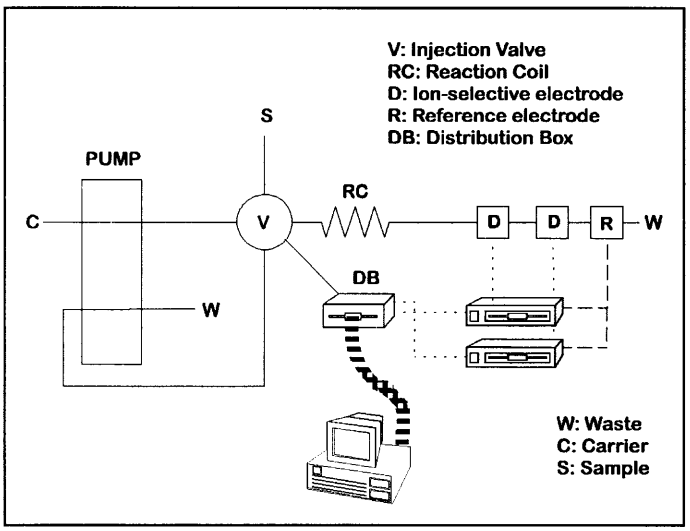

Figure 1. Components of the flow injection system.

CLFMANIF.WPG

Flow injection subsystem

This subsystem used the same components as mentioned in the previous chapter, except for the changes mentioned below.

The flow cell used at first was the same as the one in the previous chapter. Later, an edge-jet cell [3] was used. This cell is of rigid construction, with a variable volume, and can be dismantled for maintenance and reassembled. It consists of two parts, a collar and a cap. The collar is clamped around the electrode body and provide a stable foundation for the cap, which is pushed over the tip of the electrode and screwed onto the collar (see Figure 2). The cavity formed by the tip of the electrode and the bottom of the cap forms the electrode cell.

To prepare the cell for use, the collar is lightly clamped around the electrode body, a nd the cap put onto the electrode tip. The screws are inserted and tightened, drawing the collar towards the tip of the electrode. When the collar and the cap abut, the bottom of

References on page - 91 -

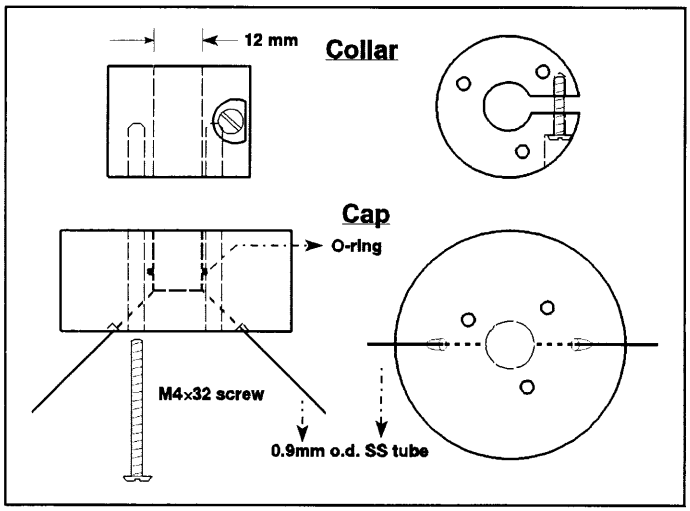

Figure 2. The edge-jet flow-through cell.

FLOWCEL3.WPG

the cap's cavity touches the tip of the electrode[1], giving a cell of minimum (zero) volume. The collar is tightly clamped, the screws extracted and the cap is removed; the cell is now ready to be used.

When the electrode is to be used the cell volume can be controlled by inserting spacers of known thickness into the space between the cap and the collar, before tightening the screws. Shim stock, readily available in a variety of thicknesses for engineering purposes, make convenient spacers. For this work a spacer of 0.5 mm was used, giving a cell volume of 66 $\mu\ell$, which, according to Davey *e.a.* [3], is close to optimum.

Injection was either by *timed injection* or by *slug injection*. Two modes of timed injection were used. In the first (switch mode), the valve switched a sample stream in the place of the carrier stream for the appropriate time (Figure 3). In the second mode of timed injection (slug mode), the configuration was as for slug injection, but with a large sample loop (Figure 4). The valve is switched to 'inject' for only long enough to let the necessary volume of sample into the manifold [4].

[1]For this reason, the bottom of the cavity should be machined completely flat. Projections could exert enough pressure to crack the membrane.

References on page - 91 -

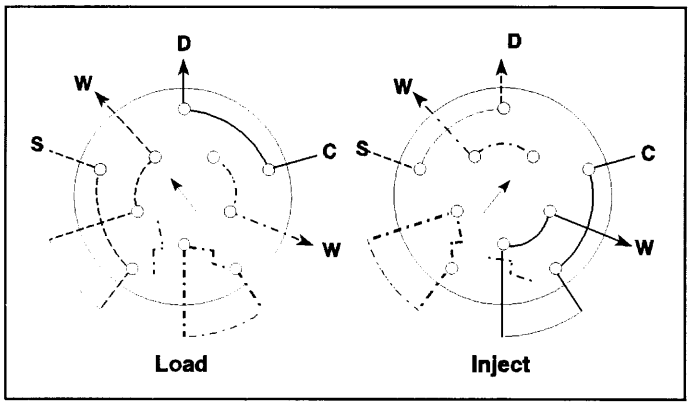

Figure 3. Valve configuration for switch mode timed-injection. TIMED1.WPG

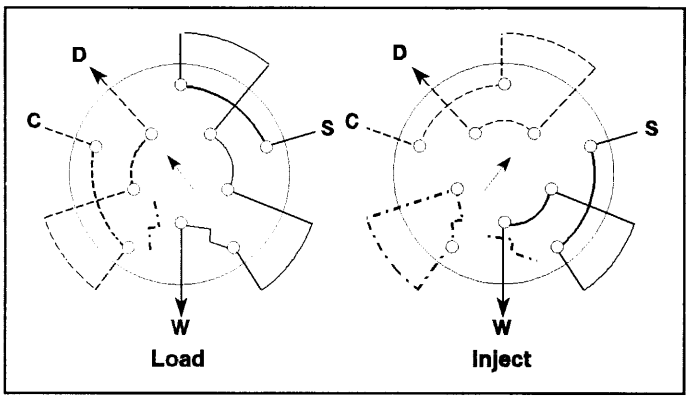

Figure 4. Valve configuration for slug-injection or slug mode timed-injection. TIMED2.WPG

Potentiometry subsystem

Potentials of an Orion (Orion Research Inc, Boston, MA) Model 94-17B Chloride electrode and a Model 94-09 Fluoride electrode were each measured by an Orion Model 901 microprocessor ionalyser. In the paragraphs that follow, the chloride electrode will be called **CL** and the fluoride electrode will be called **FL**.

The chart recorder output of the Ionalysers were amplified by inverting amplifiers supplied by Mintek (Randburg, South Africa). The signal was further amplified by the FlowTEK distribution board. This double amplification gives a total gain of −32.8 over the electrode potentials.

References on page - 91 -

The reference electrode was the double-junction Model 90-02 Ag/AgCl electrode with the outer chamber filled with carrier solution. With carrier solution in the outer chamber only the inner junction generates a junction potential, while contamination of the sample by inner chamber solutions is avoided.

All measurements were made at room temperature, which was maintained between 20 °C and 25 °C.

Control & data collection subsystem

Besides the components described in the previous chapter, the program Wave View for Dos 1.19 (Eagle appliances, Cape Town, South Africa) was used to collect and analyse potential data.

4.2.2 **Reagents**

Reagents for the carrier stream:

$NaNO_3$, (extra pure, Merck)

$Na_3C_6H_5O_7 \cdot 2H_2O$ (sodium citrate dihydrate), (AR, Protea)

DCTA (trans-1,2-Diaminocyclohexane-N,N,N',N'-tetraacetic acid monohydrate, (purum p.a. for complexometry, Fluka)

The carrier solution was prepared by mixing sodium nitrate (42.4963 g), sodium citrate (24.4988 g) and DCTA (2.6419 g) with water. The mixture was heated in a microwave oven to aid dissolution, and transferred to a 1 ℓ volumetric flask. To this was added fluoride (5 ml of a 10 mgℓ^{-1} NaF solution) and chloride (1 ml of a 1000 mgℓ^{-1} NaCl solution), before filling up to the mark.

This gives a solution with pH 5.9 and ionic strength 1.058 molℓ^{-1}, 1.0 mgℓ^{-1} Cl^-, and 0.05 mgℓ^{-1} F^-.

Reagents for preparing standards:

Chloride: NaCl (AR, Associated Chemical Enterprises)

References on page - 91 -

Fluoride: NaF (UNIVAR, Saarchem)

A stock solution of 12 500 mgℓ^{-1} Cl^- was prepared by dissolving 5.1580 g of NaCl in 250 mℓ of water.

The fluoride stock solution (75 mgℓ^{-1}) was prepared by dissolving 1.0355 g of NaF in 250 mℓ of water, and diluting 10 mℓ of this solution to 250 mℓ.

Standards with concentration ranging from 10 to 250 mgℓ^{-1} (Cl^-) and 0.09 mgℓ^{-1} to 1.5 mgℓ^{-1} (F^-) were prepared by appropriate dilution of the stock solutions.

4.2.3 **Calibration**

A program, written in Microsoft QBasic V1.1, was used to determine the baseline and peak height. It finds the modus of the data in the profile file, which is the baseline. The peak height is simply the maximum of the data. Peak height, the difference between the peak maximum and baseline, is used as concentration predictor.

The usual method for calibrating electrodes is linear calibration. When ISEs are used to measure ions at low concentrations, the electrode response is not linear. Simpson's suggestion [5] that a quadratic equation be used to calibrate was investigated, and found adequate. The concentration was regressed on the peak height using the equation.

$$R = R_0 + S_1 \cdot \log(c) + S_2 \cdot (\log(c))^2$$

References on page - 91 -

4.3 RESULTS AND DISCUSSION

4.3.1 Preliminaries

A preliminary study was carried out to test the basic assumption of this work: is the mutual interference of the chloride and fluoride electrodes negligible? An unoptimized system with a 1 molℓ^{-1} $NaNO_3$ carrier solution was used.

Two calibration curves were constructed for each electrode. In the first, a 'diagonal' calibration is done: the concentration of interfering ion is varied in the same direction as the primary ion. For the second calibration curve the interfering ion concentration is kept constant.

The calibration curves for **CL** are given in Figure 5.

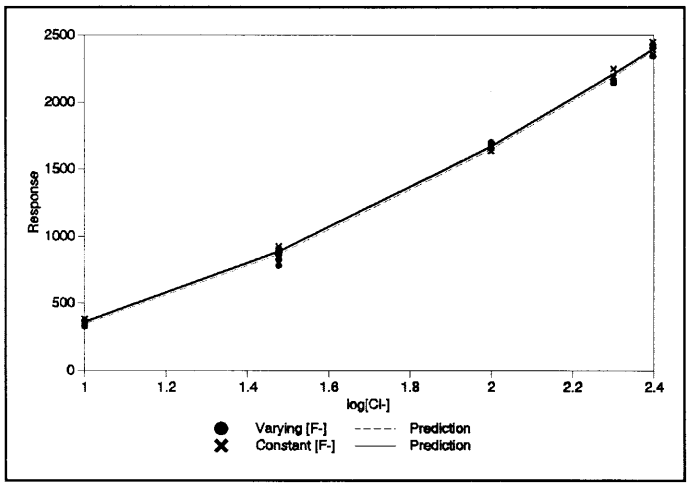

Figure 5. Calibration of chloride electrode. CLCOMP.WPG

Using 10, 30, 100, 200 and 250 mgℓ^{-1} Cl^- and 0.09, 0.3, 0.6, 0.9 and 1.5 mgℓ^{-1} F^- respectively, the following parameters were obtained:

R_0 = −167.57 S_1 = 115.041 S_2 = 395.1638 R^2 = 0.997

Using 10, 30, 100, 200 and 250 mgℓ^{-1} Cl^- but a constant fluoride concentration of 1.5 mgℓ^{-1} F^-:

R_0 = −182.42 S_1 = 163.107 S_2 = 381.4095 R^2 = 0.995

References on page - 91 -

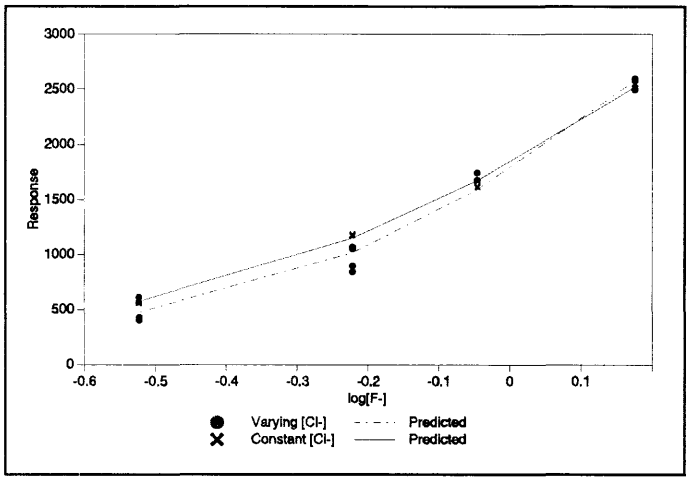

Figure 6. Calibration of fluoride electrode. FCOMP.WPG

As was expected, these results show that the fluoride concentration is too low and the range too small to have much influence on the chloride calibration.

The calibration curves for **FL** using 0.3, 0.6, 0.9 and 1.5 $mg\ell^{-1}$ F^- and 30, 100, 200 and 250 $mg\ell^{-1}$ Cl^- are shown in Figure 6

R_0 = 1767.897 S_1 = 4075.62 S_2 = 3054.832 R^2 = 0.986

With 0.3, 0.6, 0.9 and 1.5 $mg\ell^{-1}$ F^- and a constant chloride concentration of 250 $mg\ell^{-1}$ Cl^- was found that:

R_0 = 1827.669 S_1 = 3543.50 S_2 = 2200.965 R^2 = 0.998

Chloride at varying concentrations seems to effect **FL** more than *vice versa*, but the difference can be explained by the variance of the measurements. An alternative explanation is the influence of a variable ionic strength of the standards (see 4.3.3, p - 76 -).

References on page - 91 -

4.3.2 **Manifold**

Flow cell

The simple cap cell performs inadequately. An electrode must be removed from its cell from time to time, and the disadvantage of the cap cell is that peaks recorded before its removal differs from the peaks recorded after its replacement. Figure 7 shows two sets of three replicate injections using the simple cap cell. After the first set, the electrode was removed from the cell, rinsed with distilled water, and replaced. (This is a simple simulation of electrode maintenance in a process analyser.) In this example it can be seen that the peak of the second is lower and wider. If a third set had been taken, it could have been higher and sharper than the first.

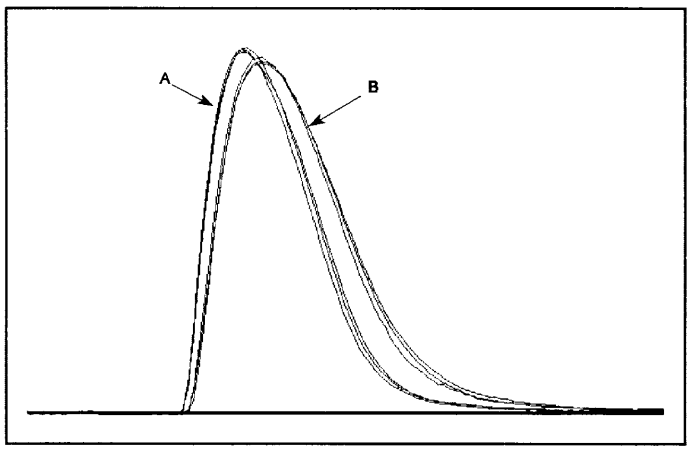

Figure 7. The cap cell: Peaks recorded before (A) and after (B) rinsing. FCBAD.WPG

When the same simulation is performed on the edge-jet cell, two improvements are visible (Figure 8). In the first place, the peak repeatability is higher, and secondly, the difference between the two replicates is much smaller. As a balance to this improvement, it should be noted that more work is needed to remove the electrode from the edge-jet cell, because the three screws must removed, and the spacers must be handled.

References on page - 91 -

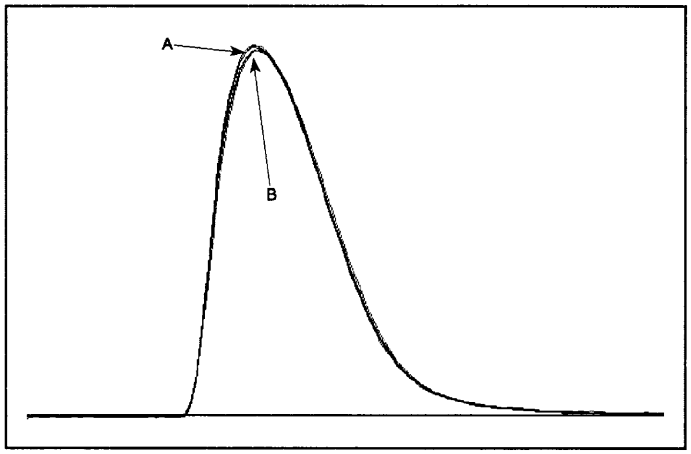

Figure 8. The edge-jet cell: Peaks recorded before (A) and after (B) rinsing the electrode. FCGOOD.WPG

A wall-jet[2] cell has superior characteristics to the edge-jet cell [6], notably in response time, but it breaks up the sample zone. The edge-jet cell is a thin-layer cell, which implies a slower response, but offers the advantage that the sample zone traverses the cell intact. The combination of intact sample zone and moderately fast response makes the edge-jet cell the preferred cell for use in electrode arrays in FIA.

The main drawback of this flow cell is that it is an efficient bubble trap. (This is a greater problem with **FL** than with **CL**; The LaF_3 seems to be more hydrophobic, and holds the bubble to its surface.) Once a bubble is trapped, no matter its size, the flow inside the cell changes and the subsequent peaks with it. The incidence of bubbles can be diminished by reducing dissolved gases in the carrier solution, trapping of bubbles and avoiding bubble entry.

Dissolved gases can be removed by degassing the carrier solution under vacuum, or by boiling it. Boiling is particularly convenient when a microwave oven is used to heat the solution.

[2] In the *wall-jet cell* the flowing electrolyte impinges perpendicularly on the active surface of the active surface of the electrode and flows radially over its surface. Under such flow conditions the static layer is very thin, causing the electrode response to be fast.

References on page - 91 -

Bubbles with an origin before or at the pump were trapped by a large-volume chamber (4 ml), with both inlet and outlet at the bottom, installed between the pump and the valve. Frenzel [7] used a porous teflon tube as de-bubbler [8]. Without disturbing the flow or dispersion, it removes bubbles before it reaches the electrode. In segmented analysers, a debubbler is used as close to the detector as possible. In FIA, it should be as close to the valve as possible, since bubbles travelling with the sample plug disturb dispersion.

Bubble entry is avoided by making sure all connections are secure and by keeping the whole system under positive pressure.

Injection mode

Timed-injection offers the advantage of equal dispersion for leading and trailing edges of the sample plug. This reduces tailing [4]. Furthermore, timed-injection makes injection volume a parameter that is easily changed: instead of replacing valve components, adjusting a number in the computer changes the sample volume.

Despite these advantages, it was decided to use slug injection. The potential dip caused by the reverse switching of the valve (see 4.3.5) was considered unacceptable, because the magnitude of its influence cannot be measured.

Switch-mode timed-injection was abandoned because of the high sample consumption. A constant flow through the detector is desirable. Therefore, during the injection, sample is pumped at the same rate as the carrier solution. If, as we have done here, a single multichannel peristaltic pump is used, this flow is maintained while the sample line is loaded, and after injection. It is unacceptably high. The problem is not the sample consumption (water samples are large and inexpensive), but that standard solutions (expensive to prepare) are consumed at the same rate.

References on page - 91 -

4.3.3 **Electrodes**

The fluoride electrode is extremely selective. There are nevertheless three kinds of interference: acid interference, metal interference and hydroxide interference. Metal and acid interferences are of secondary nature, *i.e.* they affect levels of free fluoride rather than interfering with ion exchange. Hydroxide is the only species that interferes directly.

Acid interference is caused by the protonation of fluoride.

$$H^+ + F^- \rightleftharpoons HF$$

Metal interferences are caused by the formation of coordination compounds by metal ions and fluoride [9], *e.g.*

$$Al^{3+}(aq) + F^-(aq) \rightleftharpoons [AlF]^{2+}(aq)$$

$$[AlF]^{2+}(aq) + F^-(aq) \rightleftharpoons [AlF_2]^+(aq)$$

$$[AlF_2]^+(aq) + F^-(aq) \rightleftharpoons [AlF_3](aq)$$

$$[AlF_3](aq) + F^-(aq) \rightleftharpoons [AlF_4]^-(aq)$$

$$[AlF_4]^-(aq) + F^-(aq) \rightleftharpoons [AlF_5]^{2-}(aq)$$

$$[AlF_5]^{2-}(aq) + F^-(aq) \rightleftharpoons [AlF_6]^{3-}(aq)$$

(Of course, from the viewpoint of the Lewis or HSAB theory, metal and acid interferences are equivalent. Note that the primary metal interferences, Fe^{3+} and Al^{3+}, are hard acids, and F^- is a hard base.)

For many years it was supposed that the hydroxide interference is caused by the low solubility of a $La(OH)_3$ layer that forms on the electrode surface:

$$LaF_3(s) + 3OH^-(aq) \rightleftharpoons La(OH)_3(s) + 3F^-(aq)$$

This reaction frees fluoride from the electrode membrane, lowering the electrode potential.

References on page - 91 -

Later work [10,11], however, showed that the mechanism is more complex than first assumed. LaF_3 is a hygroscopic substance, and on exposure to air or water, the outer 20 nm hydrates to $LaF_3 \cdot 3H_2O$. This layer allows the migration of F^- but any other ion that can penetrate this layer will interfere with the fluoride-exchange process. The only species that will do this is OH^-. Additionally, a slow ageing process of the membrane produces a 5 nm layer of $LaF_{3-n}(OH)_n \cdot mH_2O$, and this is presumably linked to the non-stoichiometric dissolution of LaF_3 [12].

Polishing the fluoride electrode surface removes this outer hydroxilated layer, exposes a fresh surface of LaF_3, and allows unimpeded transfer of fluoride to and from the solution.

Regular polishing of the fluoride electrode is necessary to maintain a sensitive and fast response [13]. Figure 9 shows the difference between the profiles provided by a polished and an unpolished fluoride electrode. Before polishing the electrode had been in use for a week. The electrode was polished with a plastic film coated with alumina particles. (This polishing paper is supplied by Orion Research for the polishing of halide-selective electrodes.)

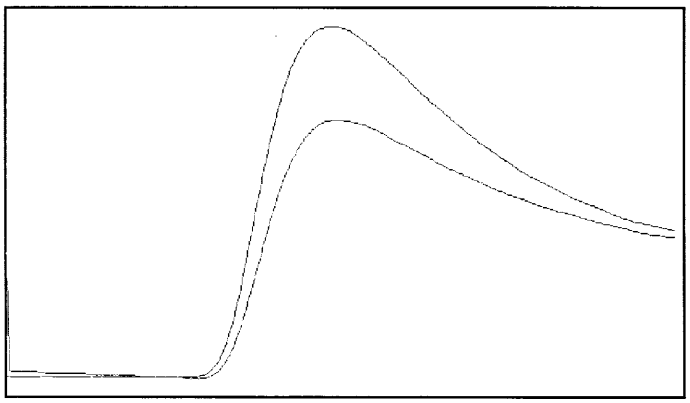

Figure 9. The improvement in electrode response after polishing. POLISH.WPG

A further benefit of polishing the fluoride electrode is the elimination of the effect of a difference in the ionic strength between standard and sample. For the peaks shown in

References on page - 91 -

Figure 10 two standards with $[F^-]$ = 1.5 mgℓ^{-1} and $[Cl^-]$ = 250 mgℓ^{-1} were prepared. The first was made up in water, the second in carrier solution (1 molℓ^{-1} $NaNO_3$ with low amounts of fluoride and chloride.) When these were injected (A), the standard with high dissolved solids gave a lower response than the one with low dissolved solids. After the electrode has been polished this difference is much reduced (B) (see Figure 10).

That this 'ionic strength interference' is different from the slower response due to deactivation of the membrane can be deduced from the fact that the electrode polished and unpolished give similar peak shapes, with similar return times. This 'ionic-strength interference' depends on the age of the electrode, and becomes apparent before the slowing of the electrode response.

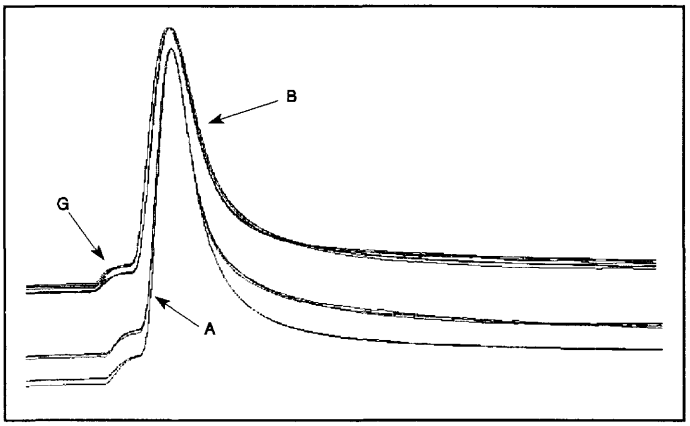

Figure 10. The effect of ionic strength difference on **FL** before (A) and after (B) polishing. G: Disturbance by valve switching. ISPOFL.WPG

The chloride electrode's response to polishing is shown in Figure 11. It can be seen that there is no difference between the two peaks, despite a change in ionic strength. The change in the peak shape of the two sets can be attributed to the change in flow pattern on reassembly of the **CL** cell (See 4.3.2, page - 72 -). The 'hump' (H) in the second set (B) is a good example of 'channelling', the existence of two paths of different length through the manifold [4], caused by a stagnant zone in the manifold.

The chloride electrode surface also deteriorates with time when used for long periods in aqueous solutions. Its colour becomes lighter, and the surface softer. This does not

References on page - 91 -

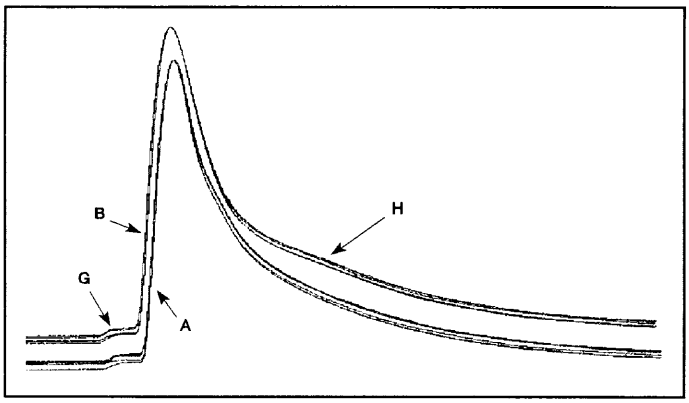

Figure 11. The effect of ionic strength difference on **CL** before (A) and after (B) polishing **CL**. G: Disturbance by valve switching. H: Hump caused by 'channelling'.

ISPOCL.WPG

appear to influence the response of the electrode.

4.3.4 **Chemistry**

After perusal of the literature it was decided to use a buffer of 1 molℓ^{-1} ionic strength, made up of citrate buffer, sodium nitrate, and DCTA. DCTA is a chelating agent specific for aluminium and iron(III), the main interferents in fluoride analysis. Hexamine-based buffer solutions, though recommended [14] for fluoride analysis, cannot be used in chloride analysis, because it rapidly erodes the electrode surface by removing Ag^+ in the form of soluble complexes.

The main interferents on the chloride electrode are species that form silver salts less soluble than AgCl. In drinking water their concentrations are too low to interfere [7].

4.3.5 **Electronics**

A disturbance on the peak profile occurred when the valve switched (Figure 12). On investigation it was found that this disturbance was caused by the earth connection of the valve. In the one position its stainless steel body earths the solution, while in the

References on page - 91 -

other it does not. Since the mechanism of this earth switching is not known, the problem was solved by breaking the *ground loop* through the valve actuator.

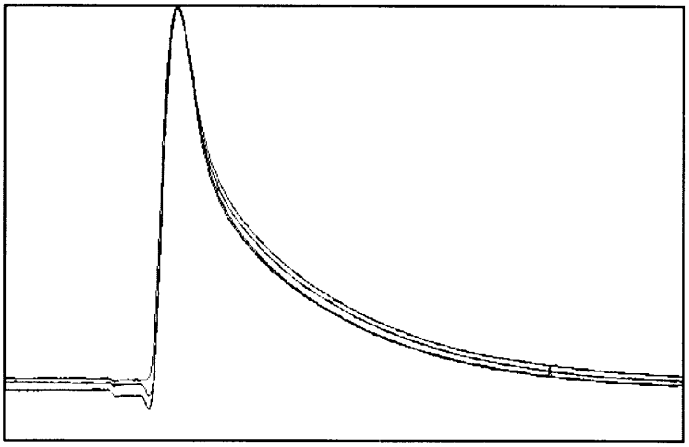

Figure 12. Peak profiles before isolation of the solution.

GNDBAD.WPG

Ground loops are created when different electronic instruments are electrically connected and each has its own earth connection [15]. A complete circuit of instrument case, connecting conductors, second instrument case and earth connection is formed. Any potential generated in this loop will cause a potential drop across the connecting conductor that may, or may not, be reflected in the measured potential. Contact potential and electrolytic action are common sources of potential, but the most troublesome are potentials induced by electromagnetic fields, commonly from the electricity supply. Ground loops are broken by connecting the cases of the instruments to each other, and earthing only one of them.

Figure 14 shows where the ground loops originated and how they were eliminated. In practice the earthing wires of both Ionalysers and the earthing wire of the valve were removed in the power plugs, and ground connections were established through the distribution box and the computer. The resulting peaks are shown in Figure 13.

Special precautions must be taken when working with earthed solutions. Orion Research [16] specifies that the reference electrode must use a low-current input into the instrument and Burton [18] states explicitly that the reference electrode should be earthed

References on page - 91 -

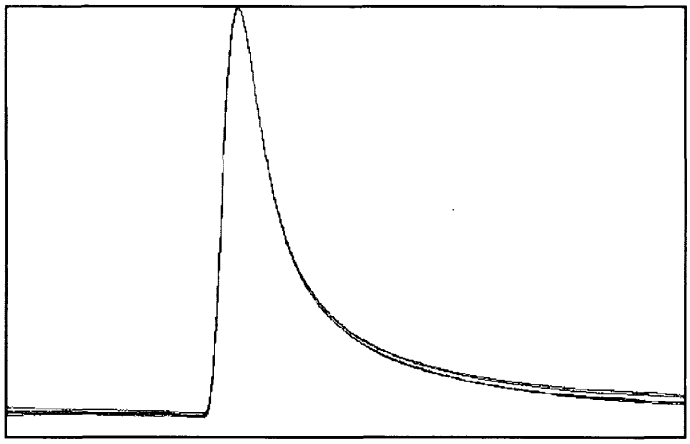

Figure 13. Peak profiles after isolation of the solution.

GNDGOOD.WPG

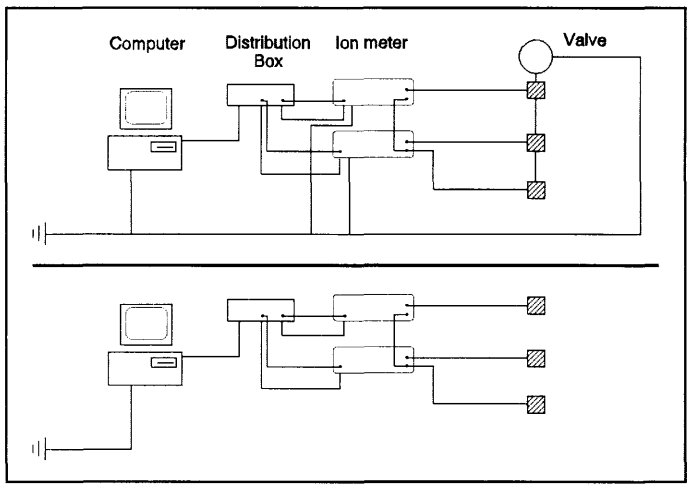

Figure 14. A setup with ground loops (top), and one without (bottom).

only if the solution is not. This must be done because the solution can be at any potential, which could make a current pass through the reference electrode. The reference electrode should be well isolated from earth [17].

Electronic solutions to these problems exist. Cammann [15] suggests using a battery powered pH meter. If a digitizer is included, it can transmit its information to the computer by an infrared link. This is an expensive and complicated option, and a much simpler solution is to separate the process solution and analysed solution by an air gap.

References on page - 91 -

In industrial flow injection analysers the only component of the analyser that might need to be at ground potential is the valve. Valves made of engineering plastics may provide enough isolation to keep the solutions in the analyser from contacting ground.

Whether it is necessary to use an earthed or a non-earthed system depends on the conditions of use, but a firm decision should be taken, and the system designed accordingly.

The 12 bit analog-to-digital converter is not optimal for ion-selective electrode work. According to Burton [18] "... an instrument for measurement with ion-selective electrodes must accept an input signal level, which may be anywhere between -900 mV and $+600$ mV, and may have a source resistance up to 4 GΩ at 0 °C. The input span for a full-scale change in reading could be 10 mV to 1 V, depending both on the ion to be selected [*sic*] and on the concentration range required." To amplify a signal 10 times to utilize to the full the precision of the analog-to-digital converter is unnecessary - it introduces complexity and distortion. Instead, an impedance converter that feeds a -1 V to $+1$ V analog-to-digital converter would be adequate.

References on page - 91 -

4.3.6 **Streaming Potentials**

From the outset of this work, it was found that the first electrode in the series (*i.e.* the electrode the sample plug reaches first) gave less repeatable profiles. On the principle that the analyte with the lower concentration should be detected first because the first electrode has a lower dispersion, this electrode was usually **FL**. The low repeatability of the peak was attributed to the low levels to be detected. Once the edge-jet cell was used, the repeatability of **FL** worsened. When the electrode order was inverted, **FL** became repeatable, and **CL** showed a periodic disturbance with a frequency suggesting an origin in the peristaltic pump. Using Wave View, the baseline was recorded for 10 seconds for each of the two orders. These are shown, highly magnified, in Figure 15 and Figure 16.

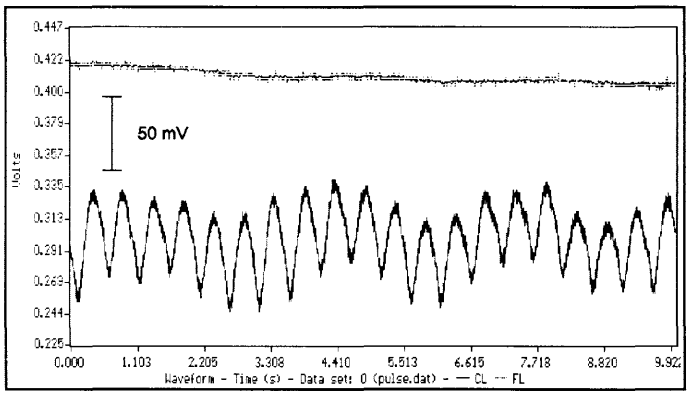

Figure 15. Baseline when the flow passes **CL** before **FL**.

PULSE.WPG

Various kinds of devices for pulse-damping were included in the manifold. These included an air chamber and a long coiled tube before the manifold, but they did not improve either pulsation or the stability of the baseline.

When the tube connecting the two cells of the array (10 cm 0.76 mm i.d. Tygon) was replaced by a 140 cm tube of the same bore, the oscillation of the first electrode's potential increased dramatically and the amplifier offset had to be adjusted to keep it on scale, but the potential oscillation of the second electrode remained constant.

References on page - 91 -

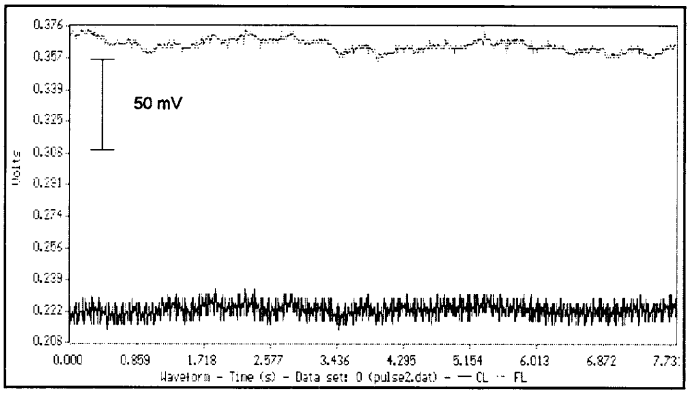

Figure 16. Baseline when the flow passes **FL** before **CL**.

PULSE2.WPG

When the carrier stream was split and each half conducted to each cell (connected to the reference electrode by a wide-bore tube) independently, the pulsation was minimal (Figure 17). These effects showed that the instability of the baseline was caused by a pressure drop in the tube leading from the indicating electrode to the reference electrode.

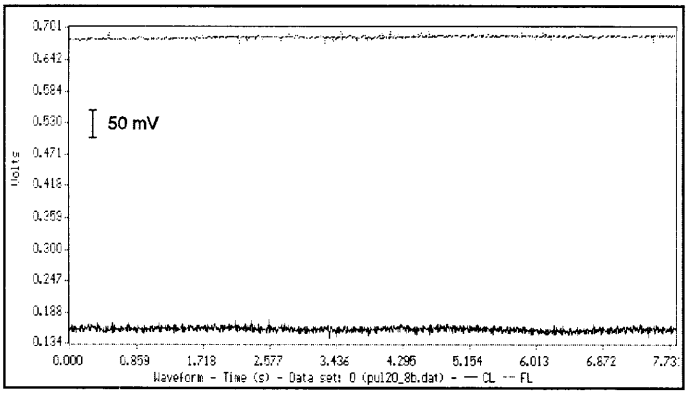

Figure 17. Baseline when the flow is split before reaching the detectors.

PUL20_8B.WPG

The periodic nature of the baseline disturbance can be attributed to streaming potentials. Van den Winkel *e.a.* [20] examined similar pulsations in an automatic fluoride analyser, and showed convincingly that it was caused by streaming potentials. A Fourier transform of Figure 15 shows peaks at 0.3 Hz, 2,4,6 and 8 Hz, and 50 Hz. The 50 Hz peak is caused by induction from the electricity supply. The diminishing series 2, 4, 6, and 8 Hz is caused by the pump rollers: at 20 rpm a pump with six rollers compresses the pump

References on page - 91 -

tube 120 times per minute, or at a frequency of 2 Hz. (The multiples of 2 are overtones.) The pump rollers are driven by a toothed belt from an electric motor. A dent visible in the flange of the driven sprocket causes the torque to be non-uniform, and is probably responsible for the 0.3 Hz component of the pulsation.

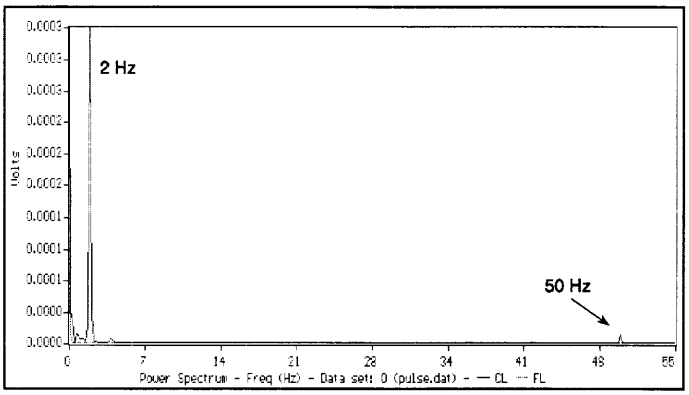

Figure 18. Fourier transform of baseline when the flow passes **CL** before **FL**. PULSEFT.WPG

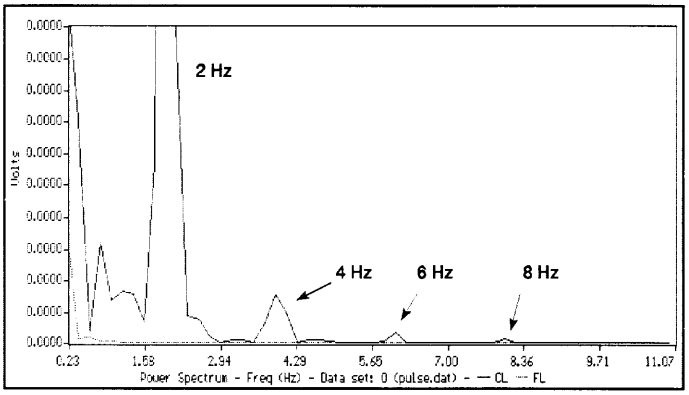

Figure 19. A portion of Figure 18 shown with expanded scales. PULSEFTZ.WPG

When the electrode order is turned around, the Fourier transform (Figure 20) of the baseline (Figure 16) shows a lower intensity of pulses for **CL**, and an increased intensity of pulses for **FL**.

When the flow is split before reaching the detectors, the Fourier transform of the baseline (Figure 23) shows that 50 Hz induction noise is the dominating periodic component of the baseline. Periodic features are still seen at 0.3 Hz and in the 2 Hz series, but these

References on page - 91 -

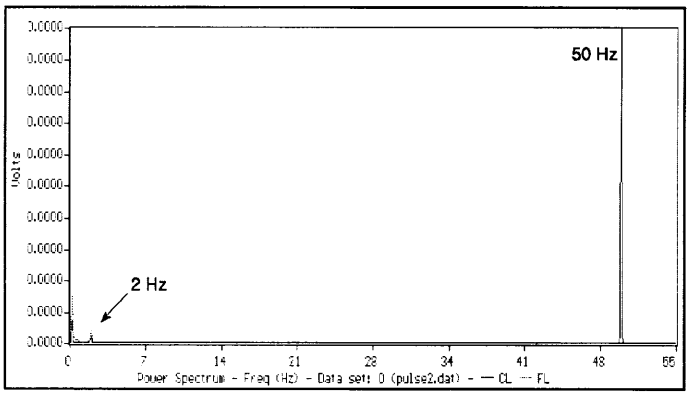

Figure 20. Fourier transform of baseline when the flow passes **FL** before **CL**. PULSE2FT.WPG

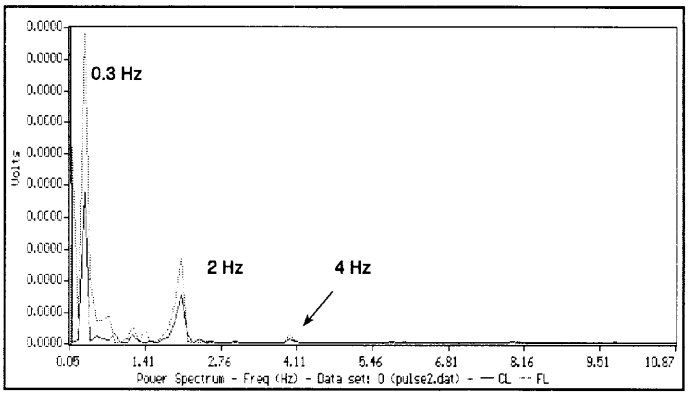

Figure 21. A portion of Figure 20 shown with expanded scales. PULSE2FZ.WPG

are comparable in intensity to peaks that do not have an obvious origin in the pump.

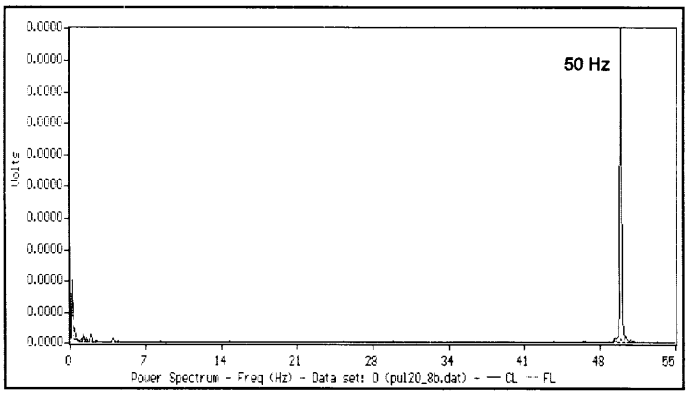

Figure 22. Fourier transform of baseline when the flow is split before reaching the detectors. PFT20_8B.WPG

References on page - 91 -

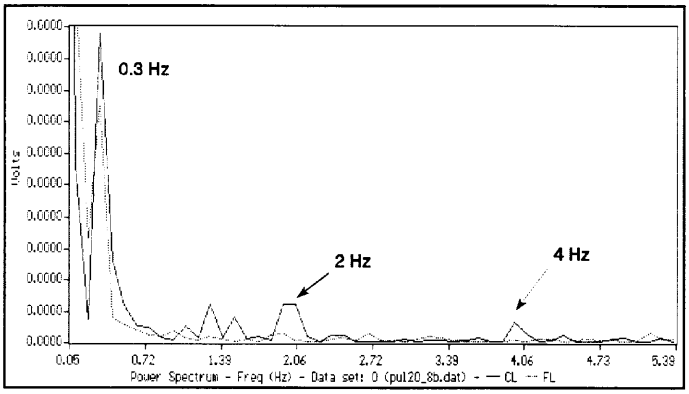

Figure 23. A portion of Figure 22 shown with expanded scales. PFZ20_8B.WPG

The difference between the size of the streaming potential for the two arrangements may be explained by the higher impedance of the fluoride electrode.

The streaming potential E_s generated between the two ends of a capillary by a liquid of viscosity η flowing with a Poiseuille velocity profile is given by the equation

$$E_s = \frac{\epsilon p \zeta}{\eta k_0}$$

where ϵ is the permittivity of the electrolyte, p is the pressure difference between the ends of the capillary, ζ is the zeta potential of the tube/electrolyte interface and k_0 is the bulk conductivity of the liquid [19].

From this equation it can be seen that the streaming potential can be reduced by increasing the viscosity or the conductivity of the liquid, or by decreasing either the pressure or the zeta potential, or both.

Adding an electrolyte to the streaming liquid will always decrease the streaming potential. It increases the conductivity and the viscosity and decreases the zeta potential.

Unfortunately the streaming potential pulsation was observed with a 1 molℓ^{-1} ionic strength solution. This is already a high ionic strength, and a further increase would be

References on page - 91 -

inconvenient because of the poor mixing of high- and low-viscosity liquids, difficulties in preparation, and higher cost.

The one remaining way to reduce the streaming potentials is by decreasing the pressure driving the flow.

Under the conditions given the pressure difference between the ends of the capillary is given by

$$p = \frac{8q\eta l}{\pi r^4}$$

The pressure difference can be reduced by decreasing the flow (q), reducing the capillary length (l), or by increasing the diameter of the capillary ($2r$). (Reducing the viscosity will also reduce the pressure, but this reduction will not affect the streaming potential. The reduction in viscosity will increase shear, which will increase the streaming potential, cancelling any improvement obtained by reducing the pressure drop.)

The *length* of the connecting tube cannot be reduced to an infinitesimal length. In this application, the length of the plastic part of the connecting tube could not be more than halved.

The solution of using a large-diameter tubing to connect the indicating electrode to the reference electrode relates to the *diameter* of the tubing. Since the pressure difference between the ends of the capillary changes with the fourth power of the capillary radius, using a 2.8 mm diameter tube instead of a 0.036 mm diameter tube reduces the streaming potential about 200-fold. This is enough to reduce the pulsation-induced streaming potential oscillation to negligible levels. Splitting the stream before it reaches the electrodes allows the use of large-bore tubes to connect each of the indicating electrodes and the reference electrode. Also, the *flow* through each cell is halved.

References on page - 91 -

Streaming potentials can be reduced by electric means. Van den Winkel *e.a.* [20] suggests earthing the ends of the capillary, or using an earthed metal connection to both cells. Another option to make the reference electrode connection in such a way that the streaming potential cancels out. These options were not considered, as the pulsation was seen as a pressure problem only.

Streaming potentials would be much less of a problem if integrated cells were used. Cells like those described by Diamond [21] have a path of a few millimetres between ISE and reference electrode. For solid state electrodes the cell design of Ferreira *e.a.* [22] could easily be extended to serial electrodes.

It is not clear why the streaming potential effects of the pulsation became problematic only when the edge-jet cells were put in use. The potential is expected to be generated by the capillary connecting the indicating and reference electrodes. These were the same for both sets of cells, and so one would expect the effects to be the same. The difference could be because the metal manifold inlet of the edge-jet cell extends into the cell cavity, and ends about 0.5 mm away from the electrode membrane, whereas in the cap cell the metal of the connector is about 5 mm away.

References on page - 91 -

4.3.7 **Achievement**

With all of the above taken into account, a system that could record highly accurate peaks was developed.

- For **CL** the peak precision of a 250 $mg\ell^{-1}$ standard was 0.85% and the electrode drift 0.6 mVh^{-1}.
- For **FL** the peak precision of a 1.5 $mg\ell^{-1}$ standard was 2.5% and the baseline drift 1.3 mVh^{-1}
- With 70 $\mu\ell$ injection volume the system could not distinguish, at a 95% level of confidence, between samples made up in water or in 1000 $mg\ell^{-1}$ $NaNO_3$.

References on page - 91 -

4.4 CONCLUSIONS

The use of electrode arrays in the simultaneous determination of non-interfering species should be carefully considered.

- Because species are to be determined together in the same system, the system parameters (e.g. sample volume) are necessarily compromise parameters.
- If the system needs to be halted for maintenance on one electrode, the information flow from all the other electrodes stops.
- The system is not naturally extendable: every species added requires further compromise.

For interfering species, these limitations are not so severe.

- Because the electrodes react similarly to the detectable species, parameters are likely to be close to the optimum of all separate systems.
- If one electrode is removed for maintenance, the information from the others is useless, so no potential information is lost. (This is not necessarily true for overdetermined systems, where more electrodes than species are used.)
- The system extends naturally towards more electrodes and more species.

For the monitoring of non-interfering species using simple parallel systems, one for each species, should be considered. Costs could be kept low by using a simple injection method such as hydrodynamic injection.

If the required sampling rate is not too high, an excellent alternative for automated analysis is sequential injection analysis (SIA). This offers many of the advantages of FIA, with the added benefit of very low reagent consumption; the only sacrifice is a lower analysis rate. The simple manifold required by ISEs suggest that a number of analyses can be done with a single selection valve. An SI analyser for the simultaneous determination of fluoride and chloride has already been developed [23].

References on page - 91 -

4.5 **REFERENCES**

1. WALDBOTT George L, *Fluoridation : The Great Dilemma* Lawrence: Coronado Press (1978) 423p. ISBN 0-87291-097-0

2. HÖLL Karl, *Wasser : Untersuchung, Beurteilung, Aufbereitung, Chemie, Bakteriologie, Virologie, Biologie*. 7., völlig neu bearb. aufl. Berlin: Walter de Gruyter (1986) 592p. ISBN 3-11-009812-1

3. DAVEY David E, MULCAHY Dennis E and O'CONNEL Gregory R, Comparison of Detector Cell Configurations in Flow-Injection Potentiometry. *Electroanalysis* (1993) **5**:581-588

4. STONE David C and TYSON Julian F, Models for dispersion in Flow Injection Analysis. Part 1. Basic requirements and Study of Factors Affecting Dispersion. *The Analyst* (April 1987) 4 **112**:515-521

5. SIMPSON RJ, Practical Techniques for Ion-Selective Electrodes. In COVINGTON AK, *Ion-selective electrode methodology*. Vol 1. Boca Raton: CRC Press (1979) vol.1 p43-66

6. FRENZEL Wolfgang and BRÄTTER Peter, The fluoride ion-selective electrode in flow injection analysis: Part 1. General Methodology. *Analytica Chimica Acta* (1986) **185**:127-136

7. FRENZEL Wolfgang, Application of flow injection potentiometry to the determination of chloride in various matrices. *Fresenius Zeitschrift für Analitische Chemie* (1989) **335**:931-937

8. MARTIN Glenn B, CHO Hee Kyoung and MEYERHOFF ME, Tubular Debubbler for Segmented Continuous-Flow Automated Analysers. *Analytical Chemistry* (November 1984) 13 **56**:2612-2613

9. Potts LW, *Quantitative Analysis: Theory and Practice.* New York: Harper & Row (1987) 710p. ISBN 0-06-045271-4

10. DE MARCO R, CATTRAL RW, LIESEGANG J, NYBERG GL and HAMILTON IC, XPS Studies of the Fluoride Ion-selective Electrode Membrane LaF_3: Ion interferences. *Surface and Interface Analysis* (August 1989) 8 **14**:457-462

11. DE MARCO R, HAUSER PC, CATTRAL RW, LIESEGANG J, NYBERG GL and HAMILTON IC, XPS Studies of the Fluoride Ion-selective Electrode Membrane LaF_3: Evidence for a Gel Layer on the Surface. *Surface and Interface Analysis* (August 1989) 8 **14**:463-468

12. TANI Yukinori, UMEZAWA Yoshio, CHIKAMA Katsumi, AKIHIDE Hemmi and SOMA Mitsuyuki, Non-stoichiometric dissolution of lanthanum fluoride (LaF_3) and its relevance to a process of ion-selective charge separation at the solid/solution interface. *Journal of Electroanalytical Chemistry* (21 November 1994) 1 **378**:205-213

13. VAN OORT WJ and VAN EERD EJJM, Effect of polishing the fluoride-selective electrode on the response time and sensitivity in flow systems. *Analytica Chimica Acta* (1983) **155**:21-27

14. CARDWELL TJ, CATTRALL RW and HAUSER PC, Buffer Systems for Use with the Fluoride Electrode in Flow Injection Analysis, *Analytical Chemistry* (January 1987) 207 **59**:206-208

15. CAMMANN K, *Working with Ion-Selective electrodes.* Translated by Albert H. Schroeder. Berlin: Springer-Verlag (1979) 226p. ISBN 3-540-09320-6

16. *Instruction Manual: Model 901 Microprocessor Ionalyser.* Cambridge MA: Orion Research Incorporated (1979) 23p.

17. MOORE F Eugene, Solving grounding problems in pH measurement. In FOWLER L,

HARMON RG and ROE DK, *Analysis Instrumentation: Proceedings of the Eleventh Annual Analysis Instrumentation Symposium* New York:Plenum Press (1965) p155-166

18. BURTON PR, Instrumentation for Ion-Selective Electrodes. In COVINGTON Arthur K, *Ion-selective electrode methodology.* Boca Raton: CRC Press (1979) vol. 1 p21-42

19. SHAW Duncan J, *Introduction to Colloid and Surface Chemistry.* 4th ed. Oxford: Butterworth-Heinemann (1992) 306p. ISBN 0-7506-1182-0

20. VAN DEN WINKEL Pierre, MERTENS John and MASSART Désiré L, Streaming Potentials in Automatic Potentiometric Systems. *Analytical Chemistry* (1974) **46**:1765-1768

21. SÁEZ DE VITERI FJ and DIAMOND Dermot, Determination and Application of Ion-selective Electrode Model Parameters Using Flow Injection and Simplex Optimization. *The Analyst* (May 1994) 5 **119**:749-758

22. FERREIRA Isabel MPLVO, LIMA José LFC and ROCHA Livio SM, Construction and evaluation of tubular potentiometric detectors sensitive to chloride, bromide, and iodide and based on homogenous crystalline membranes. *Fresenius Journal of Analytical Chemistry* (1993) **347**:314-319

23. ALPÍZAR Jesús, CRESPÍ Antonio, CLADERA Andreu, FORTEZA Rafael and CERDÀ Victor, Simultaneous Determination of Chloride and Fluoride Ions in Waters by Sequential Injection Analysis. *Electroanalysis* (1996) 11 **8**:1051-1054

Appendix 1

The Chemical Potential

Most derivations of equations expressing electrical potential as a function of solution composition start with the assertion that

$$\mu_i = \mu_i^\circ + RT \ln a_i$$

What follows here is a derivation of this expression from basic thermodynamics.

The Gibbs function describes the amount of non-expansion work a thermodynamic system can do at constant pressure:

$$G = H - TS$$

It can be shown that

$$dG = Vdp - SdT$$

Integrate:

$$\int_{G_i}^{G_f} dG = \int_{p_i}^{p_f} Vdp - \int_{T_i}^{T_f} SdT$$

If the change takes place at a constant temperature $T_f = T_i$, the second term of the integral disappears and

$$G_f - G_i = \int_{p_i}^{p_f} Vdp$$

If an ideal gas is used then $V = nRT/p$

$$G_f = G_i + nRT\int_{p_i}^{p_f}\frac{dp}{p}$$

$$G_f = G_i + nRT\ \ln\frac{p_f}{p_i}$$

The chemical potential is defined as $\mu = (\partial G/\partial n)_{pT}$:

$$\frac{\partial G_f}{\partial n} = \frac{\partial G_i}{\partial n} + RT\ln\frac{p_f}{p_i}$$

$$\mu_f = \mu_i + RT\ln\frac{p_f}{p_i}$$

If the initial conditions are standard conditions, then the chemical potential of an ideal gas at any pressure is

$$\mu = \mu^\circ + RT\ln\frac{p}{p^\circ}$$

Take a pure compound B, and mark its properties with an *

$$\mu_B^* = \mu_B{}^\circ + RT\ln\frac{p_B^*}{p_B{}^\circ}$$

$p_B{}^*$ is the vapour pressure of the pure compound. When the compound is dissolved, the chemical potential changes, but the expression stays the same.

$$\mu_B = \mu_B{}^\circ + RT\ln\frac{p_B}{p_B{}^\circ}$$

Subtract the two equations

$$\mu_B - \mu_B^* = RT(\ln \frac{p_B}{p_B^\circ} - \ln \frac{p_B^*}{p_B^\circ})$$

$$\mu_B = \mu_B^* + RT \ln \frac{p_B}{p_B^*}$$

Ideal solutes satisfy Henry's Law, which gives the vapour pressure of a solute:

$$p_B = \kappa_B x_B$$

where x_B is the mole fraction
and κ_B an empirical constant

Then

$$\mu_B = \mu_B^* + RT \ln \frac{\kappa_B}{p_B^*} + RT \ln x_B$$

Because κ_B and p_B^* are properties of the solutes this equation can be simplified to

$$\mu_B = \mu_B^\dagger + RT \ln x_B$$

where $\mu_B^\dagger = \mu_B^* + RT \ln \kappa_B/p_B^*$

When working with real solutions, deviations appear. The fraction x_B is therefore replaced by an apparent concentration a_B, called the activity.

$$\mu_B = \mu_B^\dagger + RT \ln a_B$$

Replace $\mu_B^\dagger$ with μ°, a standard chemical potential, and the equation becomes, in general,

$$\mu_i = \mu_i^\circ + RT \ln a_i$$

It is usual to use an activity coefficient f_i to link activity and concentration.

$$a_i = f_i x_i$$

Where $f_i \rightarrow 1$ as $x_i \rightarrow 0$

All deviations from ideality are captured in the activity coefficient.

For non-electrolytes the activity coefficients differ only slightly from 1. However, significant deviations appear at moderate electrolyte concentrations, caused by the high electric charge of ions. The Debye-Hückel theory describes the influence of the strong ion-ion interactions on the activity coefficient.

$$\log f_{\pm} = -\frac{|z_+ z_-| A I^{1/2}}{1 + B I^{1/2}}$$

I is the ionic strength

$$I = \frac{1}{2} \sum_i c_i z_i^2$$

A and B are empirical constants: Both depend on the medium and temperature, and B also depends on the ionic species, and is a measure of the influence of ionic radius.

The Debye-Hückel theory is of limited use in electroanalysis. It is derived for a single electrolyte only, and is only reliable at concentrations below 0.1 M. It nevertheless explains most of the reasons for the decrease in ion activity with increasing ionic strength.

It should be noted that this is strictly valid only for reversible reactions.

Appendix 2

Description of the Lotus 123 Simplex Optimizer Macro.

A "macro" in Lotus 123 is a way of automating actions normally done by pressing keys on the keyboard. In addition, a few commands can be executed, forming a simple but powerful programming language.

Simplex optimisation has been adequately described in literature, and this will not be an introduction to it.

To implement the simplex optimization, the spreadsheet program Lotus 123 was used.

The layout of this spreadsheet may seem confusing, but it must be borne in mind that it was never developed to its full extent, and never meant to be a consumer product. In fact, it was intended only as a test for the algorithm, but was found to perform sufficiently well to be used in calibration.

On the spreadsheet, three blocks are visible. The first, on the left at top, contains the experimental values, and its comparison with the modelled values. Below that is the vertices of the simplex, and other values concerning the size and motion of the simplex. To the right of and below that comes the four columns of macro lines that implement the rules for the motion of the simplex. Extending to the bottom of the sheet is a list of the best vertices of the simplex, and the size of the last step taken.

The data block:

The first three values, "E"[A3], "S"[B3], and "K"[C3], are the three values to be optimized.

The two columns of figures below "E" and "S" [A-B,5-29] contains the concentrations of chloride and bromide in the standards . The column below "K" [C,5-29] is the observed peak heights of each of the standards, and the following column [D,5-29] contains the peak heights predicted by the model. The squares of the residuals follow in the next column [E,5-29]. At the foot of this column is its sum [E30]; this is the value to be minimized. The object of macro is to find the values of E, S, and K, for which the sum of squared residuals is a minimum.

The simplex block:

Below these columns of data are a few open lines, and then four rows of the current simplex [B-D,35-38] (headed by the label "Hoekpunte"). The four vertices of the simplex is sorted from worst (least desirable response) to best (most desirable response), indicated by the labels "Slegste" and "Beste" on the left. The new vertex, labelled "Nuwe", follows in the next row [B-D,39]. To the right of the three columns describing the simplex is the response of each vertex [E,35-39].

The macro block:

The macro written to do the simplex optimization works in the following manner:

The macro is activated by pressing <ALT><G> on the computer keyboard. This transfers control to the labels in the column marked "Simplex" [G41]. {INDICATE} switches display off, and {BREAKOFF} protects the macro from untimely interruptions. The vertices are sorted {\S} by the macro labelled "Sorteer"[K45]; the new vertex is copied to the three cells [A-C,3] at the head of the data column, and the response calculated {\B} by the macro "Bereken". Next follows three conditional statements:

"A"[G42]: If the response improves from the previous best [E29<F29], the previous best [F29] is replaced by this one [E29]. The expansion factor is then set to a value greater

than unity [G38 = 2]. The subroutine "Stretch" [G53] then decides whether the expanded reflection gives a better response than the simple reflection, and allows the best step to be made.

"B"[G43]: If the objective function is not better than the previous best, but better than the second best, the next step is a simple reflection with no expansion made by the subroutine "Step" [G59].

"C"[G44]: If the response is not worse than the previous worst, the expansion factor is set smaller than unity and a step made.

If none of these conditions were met, it means that the new response is worse than at any of the existing vertices; the expansion factor is then set to a negative value [G38 = -0.7]. When a reflection is now made, the new vertex is inside the hypervolume defined by the previous simplex.

If the response at the new vertex is still not improved, it means that the simplex is too large to improve by stepping, and *the whole simplex is shrunk* (using the subroutine "Halfeer") by putting each new vertex halfway [G38] on the line connecting the best response vertex and the existing vertex. The macro is then restarted from "Simplex"

The initial vertices of the simplex are determined as follows:
In three cells [F-H,5] to the right of the data columns are functions that generate random numbers in the range that the optimum is expected to be. The variable cells are linked to these cells. When the macro "\X" is activated, the current squared sum of residuals is compared to one previously stored just below it [E31]. Normally, it is not better, so it branches back to the start of the macro. In the case that the response improves, the

values are copied to the bottom of the range, and the previously stored response replaced with the better one. The macro then starts again. The loop has no escape, and must be broken manually. Automatic recalculation must be switched off for the macro to function correctly. The final four rows are used as the initial simplex.

The initial vertices can also be random integers, typed in before the simplex is started.

Listing of spreadsheet entries.

```
F1: U +E31
O1: U 10
P1: U 10
Q1: U 0.3906
R1: 0.5981254615
A2: U ^E
B2: U ^S
C2: U ^K
O2: U 10
P2: U 50
Q2: U 1.0425
R2: 0.9145743825
A3: U -0.6023102708
B3: U 0.4582590525
C3: U 40.644442397
D3: (S2) U 0.1137343314
O3: U 10
P3: U 250
Q3: U 1.2231
R3: 1.2341025645
A4: +F6
B4: +G6
C4: +H6
O4: U 10
P4: U 1000
Q4: U 1.5137
R4: 1.5098551981
A5: U 10
B5: U 10
C5: U 0.3906
D5: +$A$3+$B$3*(@LOG(A5+$C$3*B5))
E5: (C5-D5)^2
F5: U @RAND*4-2
G5: U @RAND*3
H5: U @RAND*4
I5: U "\X
J5: U '{PANELOFF}
O5: U 10
P5: U 5000
Q5: U 1.8311
R5: 1.8301253631
A6: U 10
B6: U 50
C6: U 1.0425
D6: +$A$3+$B$3*(@LOG(A6+$C$3*B6))
E6: (C6-D6)^2
F6: U @RAND*4-2
G6: U @RAND*3
H6: U @RAND*4
J6: U '{IF E30<E31}{BRANCH J9}
A7: U 10
B7: U 250
C7: U 1.2231
D7: +$A$3+$B$3*(@LOG(A7+$C$3*B7))
E7: (C7-D7)^2
F7: U 0.0122527555
G7: U 2.5334293738
H7: U 1.6635166686
J7: U '{CALC}{BRANCH J5}
O7: U 50
P7: 10
Q7: 0.5322
R7: 0.6163783112
A8: U 10
B8: U 1000
C8: U 1.5137
D8: +$A$3+$B$3*(@LOG(A8+$C$3*B8))
E8: (C8-D8)^2
F8: U -1.5860749353
G8: U 2.1218297586
H8: U 2.0531839021
O8: U 50
P8: 50
Q8: 1.04
R8: 0.9184347934
A9: U 10
B9: U 5000
C9: U 1.8311
D9: +$A$3+$B$3*(@LOG(A9+$C$3*B9))
E9: (C9-D9)^2
F9: U -1.2516009957
G9: U 0.0730148654
H9: U 1.5909684952
J9: U '{GOTO}F5~
O9: U 50
P9: 250
Q9: 1.2451
R9: 1.2348837145
A10: U 50
B10: 10
C10: 0.5322
D10: +$A$3+$B$3*(@LOG(A10+$C$3*B10))
E10: (C10-D10)^2
F10: U -1.3998900857
G10: U 0.0187082032
H10: U 3.6590926498
J       1       0       :                       U
'/RV.{RIGHT}{RIGHT}~{END}{DOWN}{DOWN}~
O10: U 50
P10: 1000
Q10: 1.5186
R10: 1.5100509175
A11: U 50
B11: 50
C11: 1.04
D11: +$A$3+$B$3*(@LOG(A11+$C$3*B11))
E11: (C11-D11)^2
F11: U -1.9114181213
G11: U 0.1137514429
H11: U 0.1961136553
J11: U '/RVE30~E31~
O11: U 50
P11: 5000
Q11: 1.814
R11: 1.83016453
A12: U 50
B12: 250
C12: 1.2451
D12: +$A$3+$B$3*(@LOG(A12+$C$3*B12))
E12: (C12-D12)^2
F12: U -1.8233833984
G12: U 0.0578208498
H12: U 0.5460474622
J12: U '{BRANCH J5}
A13: U 50
B13: 1000
C13: 1.5186
D13: +$A$3+$B$3*(@LOG(A13+$C$3*B13))
E13: (C13-D13)^2
F13: U -1.9449746013
G13: U 0.0192840609
H13: U 0.9416402187
O13: U 250
P13: 10
Q13: 0.6836
R13: 0.6886961987
A14: U 50
B14: 5000
C14: 1.814
D14: +$A$3+$B$3*(@LOG(A14+$C$3*B14))
E14: (C14-D14)^2
O14: U 250
P14: 50
Q14: 1.0229
R14: 0.9366876431
A15: U 250
B15: 10
C15: 0.6836
D15: +$A$3+$B$3*(@LOG(A15+$C$3*B15))
E15: (C15-D15)^2
O15: U 250
P15: 250
Q15: 1.2329
R15: 1.2387441253
A16: U 250
B16: 50
```

```
C16: 1.0229
D16: +$A$3+$B$3*(@LOG(A16+$C$3*B16))
E16: (C16-D16)^2
O16: U 250
P16: 1000
Q16: 1.5039
R16: 1.5110266375
A17: U 250
B17: 250
C17: 1.2329
D17: +$A$3+$B$3*(@LOG(A17+$C$3*B17))
E17: (C17-D17)^2
I17: U "\V
J17: U '{GOTO}F5~
O17: U 250
P17: 5000
Q17: 1.8311
R17: 1.8303602494
A18: U 250
B18: 1000
C18: 1.5039
D18: +$A$3+$B$3*(@LOG(A18+$C$3*B18))
E18: (C18-D18)^2
J18: U '{FOR K18,1,3,1,J29}
K18: U 3
A19: U 250
B19: 5000
C19: 1.8311
D19: +$A$3+$B$3*(@LOG(A19+$C$3*B19))
E19: (C19-D19)^2
J19: U '{IF E25<E26}{BRANCH J25}
O19: U 1000
P19: 10
Q19: 0.9424
R19: 0.8403453978
A20: U 1000
B20: 10
C20: 0.9424
D20: +$A$3+$B$3*(@LOG(A20+$C$3*B20))
E20: (C20-D20)^2
J20: U '{CALC}{BRANCH J17}
O20: U 1000
P20: 50
Q20: 1.0693
R20: 0.9932382314
A21: U 1000
B21: 50
C21: 1.0693
D21: +$A$3+$B$3*(@LOG(A21+$C$3*B21))
E21: (C21-D21)^2
O21: U 1000
P21: 250
Q21: 1.228
R21: 1.2525882925
A22: U 1000
B22: 250
C22: 1.228
D22: +$A$3+$B$3*(@LOG(A22+$C$3*B22))
E22: (C22-D22)^2
O22: U 1000
P22: 1000
Q22: 1.5063
R22: 1.5146435665
A23: U 1000
B23: 1000
C23: 1.5063
D23: +$A$3+$B$3*(@LOG(A23+$C$3*B23))
E23: (C23-D23)^2
O23: U 1000
P23: 5000
Q23: 1.814
R23: 1.8310924875
A24: U 1000
B24: 5000
C24: 1.814
D24: +$A$3+$B$3*(@LOG(A24+$C$3*B24))
E24: (C24-D24)^2
A25: U 5000
B25: 10
C25: 1.04
D25: +$A$3+$B$3*(@LOG(A25+$C$3*B25))
E25: (C25-D25)^2
O25: U 5000
P25: 10
Q25: 1.04
R25: 1.1083303276
A26: U 5000
B26: 50
C26: 1.1426
D26: +$A$3+$B$3*(@LOG(A26+$C$3*B26))
E26: (C26-D26)^2
O26: U 5000
P26: 50
Q26: 1.1426
R26: 1.1606547297
A27: U 5000
B27: 250
C27: 1.2695
D27: +$A$3+$B$3*(@LOG(A27+$C$3*B27))
E27: (C27-D27)^2
O27: U 5000
P27: 250
Q27: 1.2695
R27: 1.3135475633
A28: U 5000
B28: 1000
C28: 1.5234
D28: +$A$3+$B$3*(@LOG(A28+$C$3*B28))
E28: (C28-D28)^2
O28: U 5000
P28: 1000
Q28: 1.5234
R28: 1.5328964162
A29: 5000
B29: 5000
C29: 1.8237
D29: +$A$3+$B$3*(@LOG(A29+$C$3*B29))
E29: (C29-D29)^2
O29: 5000
P29: 5000
Q29: 1.8237
R29: 1.8349528984
E30: @SUM(E5..E29)
F30: U 0.1137343314
E31: (D55-C55)*(C55-D55)
J54: U '/RVF5.H5~F15~
J55: U '{CALC}
A56: 'Los oop
J56: U '{BRANCH J17}
C58: ^Hoekpunte
F58: 'Sentroïed van hipervlak
A59: 'Slegste
B59: U -0.6023102708
C59: U 0.4582590525
D59: U 40.644442397
E59: 0.1137343314
F59: @SUM(B60..B62)/3
G59: @SUM(C60..C62)/3
H59: @SUM(D60..D62)/3
I59: U 1.0265926359
B60: U -0.6023102708
C60: U 0.4582590525
D60: U 40.644442397
E60: 0.1137343314
F60: 'Sentroïed van simpleks
B61: U -0.6023102708
C61: U 0.4582590525
D61: U 40.644442397
E61: 0.1137343314
F61: @SUM(B59..B62)/4
G61: @SUM(C59..C62)/4
H61: @SUM(D59..D62)/4
J61: U 'Bereken
K61: U '/RVN~I~{CALC}
A62: 'Beste
B62: U -0.6023102708
C62: U 0.4582590525
D62: U 40.644442397
E62: 0.1137343314
F62: 'Rekfaktor
G62: U -0.7
A63: 'Nuwe
B63: U +F59*(1+$A)-$A*B59
C63: U +G59*(1+$A)-$A*C59
D63: U +H59*(1+$A)-$A*D59
E63: (S2) U +R
F63: 'Kleinsimplex
G63: U 0.5
```

```
J63: U 'Ruil
K63: U '{PANELOFF}
M63: U 'Ruil slegste & 2e slegste
B64: (S2) @STD(B59..B62)
C64: (S2) @STD(C59..C62)
D64: (S2) @STD(D59..D62)
E64: (S2) @STD(SKEY)
K64: U '/RVSLEG~OOP~
M64: U ' hoekpunte uit
A65: 'Kleiner
B65: U +B$62*(1-$B)+$B*B59
C65: U +C$62*(1-$B)+$B*C59
D65: U +D$62*(1-$B)+$B*D59
F65: U "Simplex
G65: '{INDICATE}{BREAKOFF}{\S}{\B}
K65: U '/RV2SLEG~SLEG~
A66: "simplex
B66: U +B$62*(1-$B)+$B*B60
C66: U +C$62*(1-$B)+$B*C60
D66: U +D$62*(1-$B)+$B*D60
F66: U "A
G66:    '{IF    R<EEN}{INDICATE    "A"}{LET
RAKS,R}{LET A,2}{CALC}{\B}{BRANCH STRETCH}
K66: U '/RVOOP~2SLEG~
A67: 'hoekpunte
B67: U +B$62*(1-$B)+$B*B61
C67: U +C$62*(1-$B)+$B*C61
D67: U +D$62*(1-$B)+$B*D61
F67: U "B
G67: '{IF R<DRIE}{INDICATE "B"}{BRANCH STEP}
K67: U '/REOOP~
B68: U +B$62*(1-$B)+$B*B62
C68: U +C$62*(1-$B)+$B*C62
D68: U +D$62*(1-$B)+$B*D62
F68: U "C
G68:    '{IF    R<VIER}{INDICATE    "C"}{LET
A,1}{CALC}{\B}{BRANCH STEP}
K68: U '{PANELON}
G69: '{LET A,-0.7}{CALC}{\B}{BREAKON}
A70: U '2SLEG
B70: U 'B36..E36
G70: '{IF R<VIER}{\B}{BRANCH STEP}
J70: U 'Sorteer
K70: U '/DSRDSPX~PSKEY~D~G
A71: U 'A
B71: U 'G38
G71: '{IF STD<1E-12}{BRANCH EINDE}
A72: U 'ALF
B72: U 'F86..F104
G72: '{BEEP}{HALFEER}{BRANCH SIMPLEX}
J72: U 'vErvang
K72: U '{APPENDBELOW REKORD,BESTE}
A73: U 'B
B73: U 'G39
G73: '{INDICATE "EINDE VAN SIMPLEKS"}
K73: U '{APPENDBELOW HALF,A}
A74: U 'BESTE
B74: U 'B38..E38
G74: '{?}{INDICATE}
K74: U '/RVN~SLEG~
A75: U 'BESTERESP
B75: U 'E38
G75: '{QUIT}
A76: U 'DRIE
B76: U 'E36
A77: U 'EEN
B77: U 'E38
F77: U "Stretch
G77: '{IF R<RAKS}{BRANCH STEP}
A78: U 'EINDE
B78: U 'G49
G78: '{LET A,1}{CALC}{\B}{BRANCH STEP}
J78: U 'Kopieer
K78: U '/RV{R 2}~I~/RVR~{R 3}~
A79: U 'HALF
B79: U 'F86..F104
A80: U 'HALFEER
B80: U 'G63
A81: U 'I
B81: U 'A3..C3
J81: U 'Onrekord
K81: U '/REREKORD~
A82: U 'KSPX
B82: U 'B41..D44
K82: U '/RNCREKORD~A110.D110~
A83: U 'N
B83: U 'B39..E39
F83: U "Step
G83: '{\E}{LET A,1}{CALC}{BREAKON}
K83: U '/REHALF~
A84: U 'OOP
B84: U 'B32..E32
G84: '{IF STD<1E-12}{BRANCH EINDE}
K84: U '/RNCHALF~F110~
A85: U 'ORD
B85: U 'F86..F104
G85: '{BRANCH SIMPLEX}
A86: U 'R
B86: U 'E30
A87: U 'RAKS
B87: U 'F30
F87: U "Halfeer
G87: '/RVKSPX~SPX~
A88: U 'REKORD
B88: U 'F86..F104
G88: '{GOTO}SPX~
A89: U 'SIMPLEX
B89: U 'G41
G89: '{\C}{D}
A90: U 'SKEY
B90: U 'E35..E38
G90: '{\C}{D}
A91: U 'SLEG
B91: U 'B35..E35
G91: '{\C}{D}
A92: U 'SPX
B92: U 'B35..E38
G92: '{\C}
A93: U 'STD
B93: U 'E40
G93: '{BEEP}
A94: 'STEP
B94: 'G59
F94: U 'Moenie {CALC}
G94: '{RETURN}
A95: U 'STRETCH
B95: U 'G53
A96: U 'TWEE
B96: U 'E37
A97: 'VIER
B97: 'E35
A98: U '\B
B98: U 'K37
A99: U '\C
B99: U 'K54
A100: U '\E
B100: U 'K48
A101: '\G
B101: 'G41
A102: '\O
B102: 'K57
A103: '\R
B103: 'K39
A104: '\S
B104: 'K46
A105: '\X
B105: 'J5
A107: '/wdr~{d}
A109: 'Rekord
F109: 'Half?
A111: U -0.6023102764
B111: U 0.4582590546
C111: U 30
D111: 0.1830792013
F111: U 1
A112: U -0.6023102764
B112: U 0.4582590546
C112: U 30
D112: 0.1830792013
F112: U 1
A113: U -0.6023102764
B113: U 0.4582590546
C113: U 30
D113: 0.1830792013
F113: U -0.7
A114: U -0.6023102764
B114: U 0.4582590546
C114: U 30
```

```
D114: 0.1830792013
F114: U -0.7
A115: U -0.6023102764
B115: U 0.4582590546
C115: U 30
D115: 0.1830792013
F115: U -0.7
A116: U -0.6023102764
B116: U 0.4582590546
C116: U 30
D116: 0.1830792013
F116: U 1
A117: U -0.6023102764
B117: U 0.4582590546
C117: U 30
D117: 0.1830792013
F117: U -0.7
A118: U -0.6023102764
B118: U 0.4582590546
C118: U 30
D118: 0.1830792013
F118: U -0.7
A119: U -0.6023102764
B119: U 0.4582590546
C119: U 30
D119: 0.1830792013
F119: U -0.7
A120: U -0.6023102764
B120: U 0.4582590546
C120: U 30
D120: 0.1830792013
F120: U 1
A121: U -0.6023102764
B121: U 0.4582590546
C121: U 30
D121: 0.1830792013
F121: U -0.7
A122: U -0.6023102764
B122: U 0.4582590546
C122: U 30
D122: 0.1830792013
F122: U -0.7
A123: U -0.6023102764
B123: U 0.4582590546
C123: U 30
D123: 0.1830792013
F123: U -0.7
A124: U -0.6023102764
B124: U 0.4582590546
C124: U 30
D124: 0.1830792013
F124: U 1
A125: U -0.6023102764
B125: U 0.4582590546
C125: U 30
D125: 0.1830792013
F125: U -0.7
```